Rewired gene interactions during development of serially homologous appendages in male and female *Drosophila*

Amber M. Ridgway[1,2], Javier Figueras Jimenez[3], Maria D. S. Nunes[1] and Alistair P. McGregor[3,*]

[1]Department of Biological and Medical Sciences, Oxford Brookes University, Oxford OX3 0BP, UK.

[2] Current address: Department of Biology and Epigenetics Institute, University of Pennsylvania, Philadelphia, PA 19104, USA.

[3]Department of Biosciences, Durham University, South Road, Durham, DH1 3LE, UK.

*Corresponding author: alistair.mcgregor@durham.ac.uk

Keywords: evolution, development, *Drosophila*, genitalia, *C15*

Abstract

Drosophila genitalia and legs are considered to be serially homologous appendages derived from a ventral appendage 'ground state' shaped by different Hox inputs. Despite their shared origin, there has been relatively little comparison between the downstream gene regulatory networks and how they may differently pattern and shape these appendages. In the pre-tarsal region of the developing leg and antennae of *Drosophila*, a combination of the transcription factors C15, Lim1 homeobox 1 (Lim1), and Al (Aristaless) are required for the development of the leg tarsal claws and antennal aristae. However, the roles and interactions of these factors in genital development, and their relationship with other leg-patterning genes, remained unexplored. Here, we investigated the expression and function of C15, Lim1, and Al in the development of male and female terminalia (genitalia and analia). We found that C15 plays distinct roles in the different sexes, repressing male clasper bristle formation while promoting bristle development in the female epiproct. Notably, unlike in the antennal and leg discs, C15, Lim1, and Al are not all co-expressed in any anal or genital structures in either sex, indicating that the interactions among these factors have diverged across serially homologous appendages. Nevertheless, we inferred regulatory interactions between C15 and other factors, including *bric a brac 2* and *Distal-less,* reflecting similarities between leg and genital development consistent with their homology. Finally, we identified a male-specific enhancer of *C15*, likely regulated by the Hox gene *Abdominal-B* (*Abd-B*), which is active in male claspers but not in the female terminalia, legs or antennae. This *C15* enhancer modularity may underpin tissue-specific regulatory logic, presumably programmed by distinct Hox inputs such as Abd-B in the genitalia, and could contribute to the diversification of serially homologous ventral appendages.

Introduction

The diversification of serially homologous structures has been a major theme during animal evolution [1, 2]. This is exemplified by the elaboration of ventral appendages in arthropods that have evolved into a 'toolkit' of functionally distinct structures, from walking legs and swimming appendages to sensory antennae, respiratory organs, spinnerets, and genitalia [1-6]. It is thought that appendage diversity is regulated by distinct Hox gene inputs as well as other differences in the underlying developmental gene regulatory networks (GRNs) [4, 5, 7, 8]. Understanding the regulation and diversification of these mechanisms is a key question in evolutionary developmental biology.

In *Drosophila,* the legs are patterned by overlapping expression domains of the transcription factors, including *homothorax* (*hth)*, *dachshund* (*dac*), and *Distal-less* (*Dll*), along the proximo-distal axis, with expression of the latter two genes overlapping in the distal tibia and tarsal segment [9] (Fig. 1). The distal part of the leg includes the tarsus composed of five tarsal segments followed by a pre-tarsal region bearing a pair of claws (Fig. 1). Development of the tarsus and pre-tarsal region is also regulated by a proximo-distal gradient of increasing Epidermal growth factor receptor activity, which results in the activation of specific transcription factor-encoding genes, including *Bar* (*B*) and *bric a brac 2* (*bab2*), in the distal tarsal segments and *C15* (also called *clawless*) in the pretarsal region [10, 11]. C15, in turn, activates *aristaless* (*al*) and *LIM homeobox 1* (*Lim1*), which feeds back to promote *C15* expression in the pretarsal region [10, 11]. Together, C15, Lim1, and Al combine to repress *B* and *bab2* in the pretarsal region, with C15 and Al cooperatively binding to directly repress *B* expression and C15 competing with the activator Dll to regulate *bab2* expression [10-13]. Loss of C15, Lim1, or Al expression in the leg results in the loss of the pre-tarsal region, including the claws [10, 11]. This trio of transcription factors are also co-expressed and required for the development of part of another ventral appendage, the aristae of the antennae [10, 11, 14, 15]. However, in developing eyes, only C15 and Lim1 are expressed in the ocellar region [10, 11, 14, 15]. Therefore, although the combinatorial expression of C15, Lim1, and Al can differ according to the developmental context, these three transcription factors are important for appendage patterning.

Classic experiments in *Drosophila* indicated that the 'ground state' state of ventral appendages was a leg-like proximal segment and distal tarsus, and suggested Hox and *hth* inputs pattern this basic structure to give rise to specific appendages, for example *Antennapedia* in the legs [16]. In the genitalia, it is thought that the posterior Hox gene *Abdominal-B* (*Abd-B*) represses leg fate and promotes genital fate [17]. Indeed, loss of *Abd-B* results in development of tarsal-like structures from the genitalia in *Drosophila* and other insects, further supporting the appendage 'ground state' model [16-18]. While excellent progress has been made in understanding how Hox genes and downstream mechanisms regulate the identity and fine-scale morphology of appendages, especially legs, wings, and halteres [19-27], much remains to be learned about the development and evolution of genital structures.

The terminalia of *Drosophila* are composed of the analia and genitalia, which develop from the genital imaginal disc [28]. This disc is composed of cells from abdominal segments A8, A9 and A10 (Fig. 1A). The analia of both sexes derive from A10 and give rise to the anal plates in males (cerci) and females (the epiproct and hypoproct) (Fig. 1A) [28-30]. In males, the genitalia, encompassing the claspers (surstyli), epandrium and internal organs including the phallus and associated structures, develop from A9 [28, 30] (Fig. 1A). In females, the genitalia, including the oviprovector, develop from A8 [28, 29]. A8 and A9 form the repressed female primordium and repressed male primordium in males and females, respectively [28] (Fig. 1A). The primordia of adult terminal structures are marked by the expression of specific genes in the genital imaginal disc. *caudal* (*cad*) and *Abd-B* mark and regulate the development of the analia and genitalia, respectively [28]. Regulation of the development of the analia and genitalia also integrates sex-specific signals to specify and pattern male and female structures [28]. During the late third larval instar (L3) and pupal stages, the cells of the anal and genital primordia divide, differentiate and undergo metamorphosis, causing these tissues to be remodelled and develop into the adult structures [28] (Fig. 1).

Comparisons of the expression of genes encoding transcription factors between genital and leg discs have revealed similarities consistent with the concept that the terminal structures are derived walking appendages [17, 31, 32]. For example, *Dll* expression in the four distal tarsal segments in the leg is reflected in the proximal domain of the clasper and throughout the cerci in the male genitalia, while overlap of *dac* and *Dll* in the first tarsal segment and part of the tibia, is similar to their expression in the distal clasper domain (Fig. 1B). Furthermore, it has recently been shown that *C15* is expressed in the developing pupal claspers [33] and downstream target genes, including *bab2*, have also previously been shown to be expressed in the claspers during at least one developmental stage [17, 33-35]. However, the relative expression, functions, and interactions of key genes that regulate distal leg development in *Drosophila* have not previously been systematically studied in the serially homologous male and female terminalia. This information is crucial to not only understanding the development of these structures but also how they have been remodelled from the ventral appendage ‘ground state’ during evolution.

Here, we investigated the expression, function, and interactions of *C15* and upstream and downstream genes in the pre-tarsal GRN during the development of male and female *Drosophila* terminalia. Our results show differences in the deployment and interactions of these genes between the development of leg and terminal structures as well as between male and female terminalia development. Our data indicate that there has been extensive rewiring of the distal leg GRN during the evolution of male and female terminal structures, and although this re-programming involves Hox gene inputs, we present evidence that it has also potentially been underpinned by enhancer modularity.

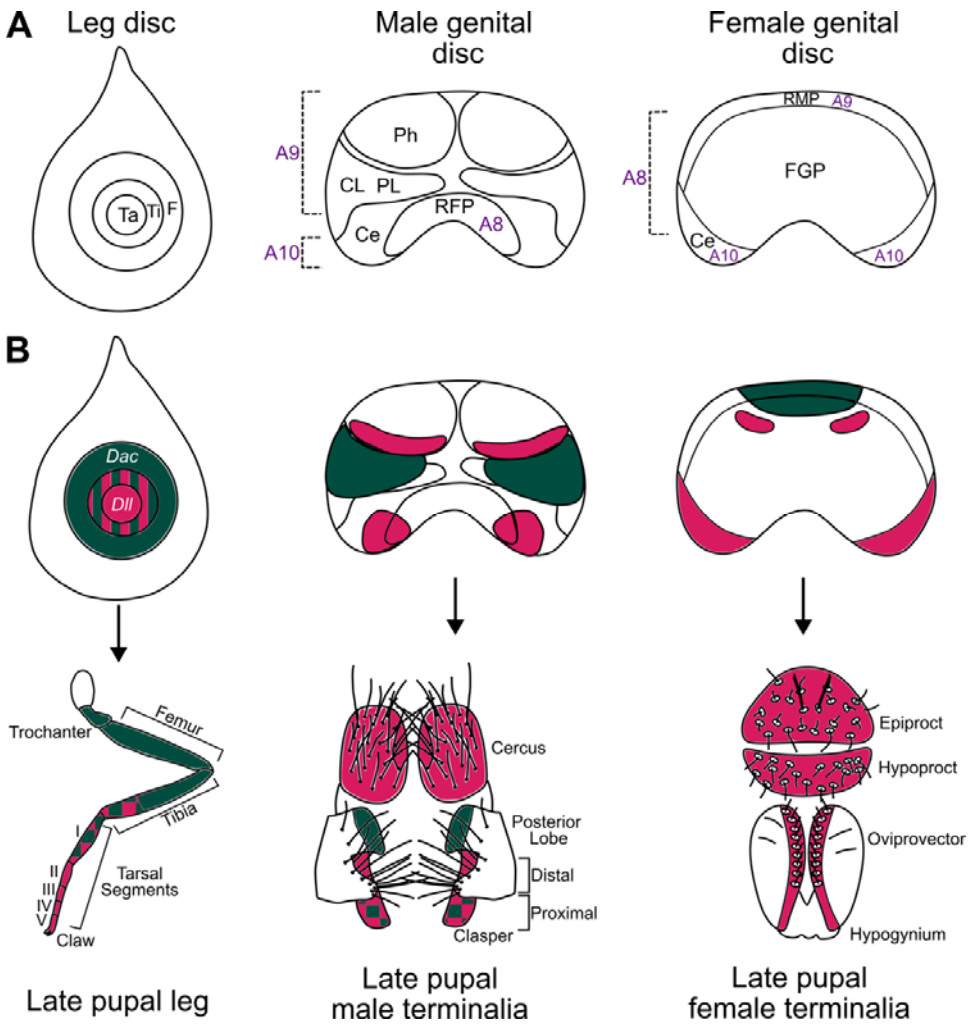

Figure 1. Development of the *Drosophila* leg and male and female terminalia. (A) Fate maps of the leg, male genital, and female genital discs. Ventral view of genital discs. The three segmental primordia of the terminalia (A8, A9 and A10) are indicated. (B) In the leg disc, *Dll* is expressed at the centre, which gives rise to the tarsal segments and distal tibia. *da*c expression marks the first tarsal segment, tibia, femur, and trochanter. In the male genital disc, *Dll* is expressed in the phallic and cercus primordia. *dac* expression in the male genital disc marks the clasper and posterior lobe primordia. During male pupal development, *Dll* is expressed throughout the claspers and cerci, and *dac* is expressed in the proximal clasper region and posterior lobe. In the female genital disc, *Dll* is expressed in the cerci primordia and part of the genital primordium. *dac* is expressed in the repressed male primordium of the female genital disc. During female pupal development, *Dll* is expressed in both anal plates and part of the external female genitalia. *dac* is not expressed in the external structures, but instead localizes to internal genital structures (not shown). Note, that the internal phallic structures are not shown in (B) for simplicity. Diagrams are not to scale. Ta: Tarsus, Ti: Tibia, F: Femur, CL: Clasper, Ph: Phallus, PL: Posterior lobe, Ce: Cercus, RFP: Repressed female primordium, FGP: Female genital primordium, RMP: Repressed male primordium. The figure summarises previously published data [9, 17, 31, 35, 36].

Materials and Methods

Drosophila lines and manipulation of gene expression

UAS-RNAi lines were provided by the Vienna *Drosophila* Resource Centre (VDRC) [37] or the Bloomington *Drosophila* Stock Centre (BDSC) (NIH P40OD018537). All *UAS-RNAi* lines used are detailed in Supplementary Table 1. *UAS-RNAi* males were crossed to *NP6333-GAL4 (P{GawB}PenNP6333)* virgin females also carrying *UAS-Dicer-2 (P[UAS-Dcr-2.D]*) [34, 37, 38]. All crosses were carried out at 25ºC. Crosses were transferred to standard cornmeal food every two days and maintained under a 12-hour light/dark cycle. Progeny were aged at least 3 days and collected and stored in 70% Ethanol (EtOH) at -20ºC.

The cerci, posterior lobes, and claspers of the adult male genitalia, and the epiproct, hypoproct, and ovipositor of adult female genitalia, were dissected using 0.14 mm diameter stainless steel pins in Hoyer's solution [39]. Dissected adult structures were mounted in Hoyer's solution on slides containing eight individual 6 mm diameter wells. To account for body size, the T2 legs of each fly were also dissected and mounted. A Zeiss Axioplan light microscope with a Jenoptik ProgRes C3 camera was used to image each dissected structure, where 250X magnification was used for the terminal structures and 160X magnification for the T2 legs. The area of the posterior lobe, cercus, lateral plate, hypoproct, epiproct and length of T2 tibia leg were measured manually using ImageJ [40]. When measuring the hypoproct and epiproct area, an outline was drawn and enclosed with an artificial baseline [41]. The bristles were counted under a light microscope using a tap counter. The area, bristle count, and length were recorded for both structures of each pair per individual, and the average was then used for the statistical analyses.

Statistical analyses

All statistical analyses were carried out using R version 4.2.0 [42]. Measurements of each structure described above were first assessed for normality using the Shapiro Wilk test. Normally distributed data were analysed using Dunnett's test and ANOVA, whereas the Kruskal Wallis test was used for non-normally distributed data [43]. RNAi knockdown progeny were compared to both parental controls. If this test was statistically significant, the Tukey's Test / Wilcoxon Rank Sum Test (BH p-adjusted method [44]) was used to identify whether the effect was significantly different to both parental controls (Supplementary Tables 1 and 2). The RNAi was considered to have had no effect if $p =/> 0.05$ or if $p < 0.05$ where the trait value in the RNAi knockdown progeny was intermediate to the two parental controls (Supplementary Tables 1 and 2). Where the T2 tibia length of the RNAi knockdown was significantly different to both parental controls following the tests described above, Pearson/Spearman correlation analysis was performed on the cercus, epiproct and hypoproct area dependent on Shapiro Wilk test results. If statistically significant, the area of the structure was divided by the tibia length squared, and statistical tests were carried out on the normalised measurements.

Scanning electron microscopy

Scanning electron microscopy (SEM) was carried out on *NP6333-GAL4* and *C15* RNAi knockdown male and female terminalia. Flies were initially stored in 70% EtOH and moved into 100% EtOH at least 24 hours prior to imaging. The posterior of the fly was dissected in 100% EtOH. Samples were processed in a critical point dryer and mounted on SEM stubs, then gold coated for 30 seconds. The terminalia were imaged using SE mode at 5 kV in a Hitachi S-3400N SEM, with a working distance of 13 to 14 mm. The entire terminalia was imaged at a magnification of 250X, and individual genital and anal structures at 900X.

Sample preparation and immunohistochemistry

Larvae were collected in ice-cold 1 X PBS, cut in half, and inverted. Larval tissues were then fixed in 4% formaldehyde in 1 X PBS for 20 minutes at room temperature. Samples were rinsed in 1 X PBS with 0.1% TRITON-X-100 (PBT) and then washed in 0.3% PBT for 30 minutes. Following this, samples were blocked for 20 minutes in 10% normal goat serum (NGS) in 0.1% PBT. Larval samples were then incubated with the primary antibody overnight at 4ºC (Supplementary Table 3). The next day samples were washed five times for 5 minutes in 0.1% PBT. The secondary antibody was added and incubated at room temperature for 2 hours. Samples were washed accordingly, DAPI stained, and then dissected on slides to isolate the required imaginal discs. Discs were mounted in VECTASHIELD and sealed with a coverslip for imaging.

Male and female white prepupae were defined as 0 hours after puparium formation (hAPF). Males were identified by two circular transparent cuticles on either side of the posterior abdomen [45], and then stored at 25 ºC until the developmental timepoint required. Using micro-scissors, staged pupae were cut near the posterior end in ice-cold 1 X PBS, then flushed with 1 X PBS to remove as much fatty tissue as possible, followed by fixation in 4% formaldehyde for 30 minutes at room temperature. Samples were washed in 1 X PBS, then gradually brought to 100% EtOH for storage at -20 ºC. Before staining, the tissues were removed from the pupal casing, leaving just the exposed genital tissue samples enclosed in the outer membrane. All steps following this were carried out in 0.3% PBT and blocked and stained in 2% NGS in 0.3% PBT. Pupal samples were blocked for 2 hours, then incubated overnight at 4 ºC with the primary antibody. The next day, pupal samples were washed for 6 x 20-minute intervals before the addition of the secondary antibody and then incubated at 4ºC overnight. Samples were subsequently washed and DAPI stained if required, then the outer membrane was removed using dissection forceps prior to mounting. Microscope slides with coverslips used as walls were used to create a well to protect the sample from being crushed during imaging. Poly-L-Lysine solution was added to the well prior to mounting to avoid movement of the tissue. All pupal samples were mounted in Hydromount and a coverslip was placed on top and sealed with nail varnish.

For all stains, the primary and secondary antibody concentrations are detailed in Supplementary Table 3. Where annotated as preabsorbed primary antibody (Supplementary Table 3), the working concentration of the primary antibody was diluted in 0.3% PBT for pupae, and 0.1% Tween-20 in 1 X PBS for larval tissues, before being incubated with inverted, fixed larvae for 1 hour at room temperature, then stored at 4 ºC.

All stained samples were imaged using a Zeiss LSM800 upright Confocal Laser Scanning Microscope. A 20X air objective was used to image larval disc samples, and a 40X oil objective for pupal samples. Some pupal structures were imaged using a 63X oil objective when capturing individual external structures. Z-stacks with 0.7 µm and 1 µm separation were used for pupal and larval samples, respectively. All images were processed with Fiji [46].

To screen for active *C15* genital enhancers, males of available GAL4 reporter lines (stock numbers BL41233, BL50056 and BL50087) [47] encompassing regions of the *C15* locus were crossed to *UAS-GFP* virgin females. To assess activity in live pupae, the outer cuticle was removed using dissection forceps, and pupae were mounted on a slide in a drop of 80% glycerol for imaging. Dorsal and ventral images were captured using Zeiss Axiozoom microscope GFP filter with Z stacks of 1 µm separation.

ATAC-seq library preparation

Prepupae were collected from *D. melanogaster* (Oregon R) and aged until 30 hAPF. Pupae were dissected in ice-cold 1 X PBS, followed by incubation in lysis buffer (10 mM Tris-HCL, pH 7.5; 10 mM NaCl; 3 mM MgCl2; 0.1% IGEPAL and 0.1% digitonin). After the lysis was stopped, the nuclei were collected by centrifuging at 500 g for 10 minutes. 50,000 nuclei were resuspended in Tagmentation Mix (25 µl tagmentation buffer (20 mM Tris-CH2COO-, pH 7.6; 10 mM $MgCl_2$; 20% Dimethylformamide); 2.5 Tn5 transposase; 22.5 µl water) and incubated for 30 minutes at 37ºC. 3 µl of 2 M NaAC, pH = 5.2 was added to the sample and then purified using a QIAGEN MinElute Kit. Library amplification was performed using NEBNext High Fidelity 2X PCR Mix with primers indexed with primers compatible with Nextera adaptors from Diagenode. 150 bp paired-end sequencing was carried out by Novogene (UK).

ATAC-seq library, peak calling and footprinting

Raw reads generated from 30 hAPF male pupae were mapped to *D. melanogaster* genome version r6.55 Dec 2023 [48] using Bowtie2 (version 2.4.5) [49]. We used Samtools (version 1.9) [50] to convert sam files to bam files and remove duplicates. Bedtools (version 2.31.1) [51] was used to convert generated data files into bed format and we re-centered the reads according to [52]. Peak calling was then performed using MACS2 (version 2.2.7.1) [53] with the parameters -extsize 50, -q 0.01. ATAC-seq datasets for *D. melanogaster* eye-antennal imaginal disc (120 hours after egg laying) and pupal T2 leg were obtained from [54] and [21], and analysed as above.

Transcription factor footprinting analysis, was carried out using the package TOBIAS (version 0.16.1) [55]. Reads were corrected using ATACorrect, which corrects the bias of Tn5 transposase for specific sequences, and this correction was then used to score regions within peaks for the likelihood of being bound by proteins. We searched for motifs within the footprints and compared them against the JASPAR core [56] and CIS-BP [57] databases to identify putative transcription factor that bind to these sites (Supplementary Tables 4 and 5).

Data availability

ATAC-seq data accession numbers: GSE279524 (pupal genital data), GSE113240 (T2 pupal leg data), and PRJNA666524 (eye-antennal-disc data).

Results

C15 *expression in developing male and female terminalia*

It was previously shown that *C15* mRNA is expressed in the proximal region of male claspers during pupal stages [33]. We examined the clasper expression of C15 further during male larval and pupal genital development by staining with anti-C15 and co-staining with anti-Odd-paired (Opa), which is known to mark the developing claspers [33] (Fig. 2A-A''). We found that C15 protein is localised to a subset of cells within the Opa-marked clasper primordium of male larval genital discs (Fig. 2A-A''). During pupal stages, C15 remains localised to the clasper but is restricted to cells in the proximal region that do not develop bristles as shown previously for *C15* mRNA expression [33] (Fig. 2B-D). In addition, C15 expression extends from the proximal domain of the claspers to the periphery of the cerci from as early as 26 hAPF (Fig. 2B-D). Throughout pupal development, C15 is also detected in the abdominal tissue dorsal of the male terminalia (Fig. 2B-D).

We next investigated C15 localisation in the developing female terminalia. In females, C15 is expressed in two well-defined cell clusters of approximately seven cells in the genital disc (Fig. 2E). This expression pattern is maintained during pupal development and surrounds the two prominent sensilla in the distal plate of the female cerci (the epiproct) (Fig. 2F,G).

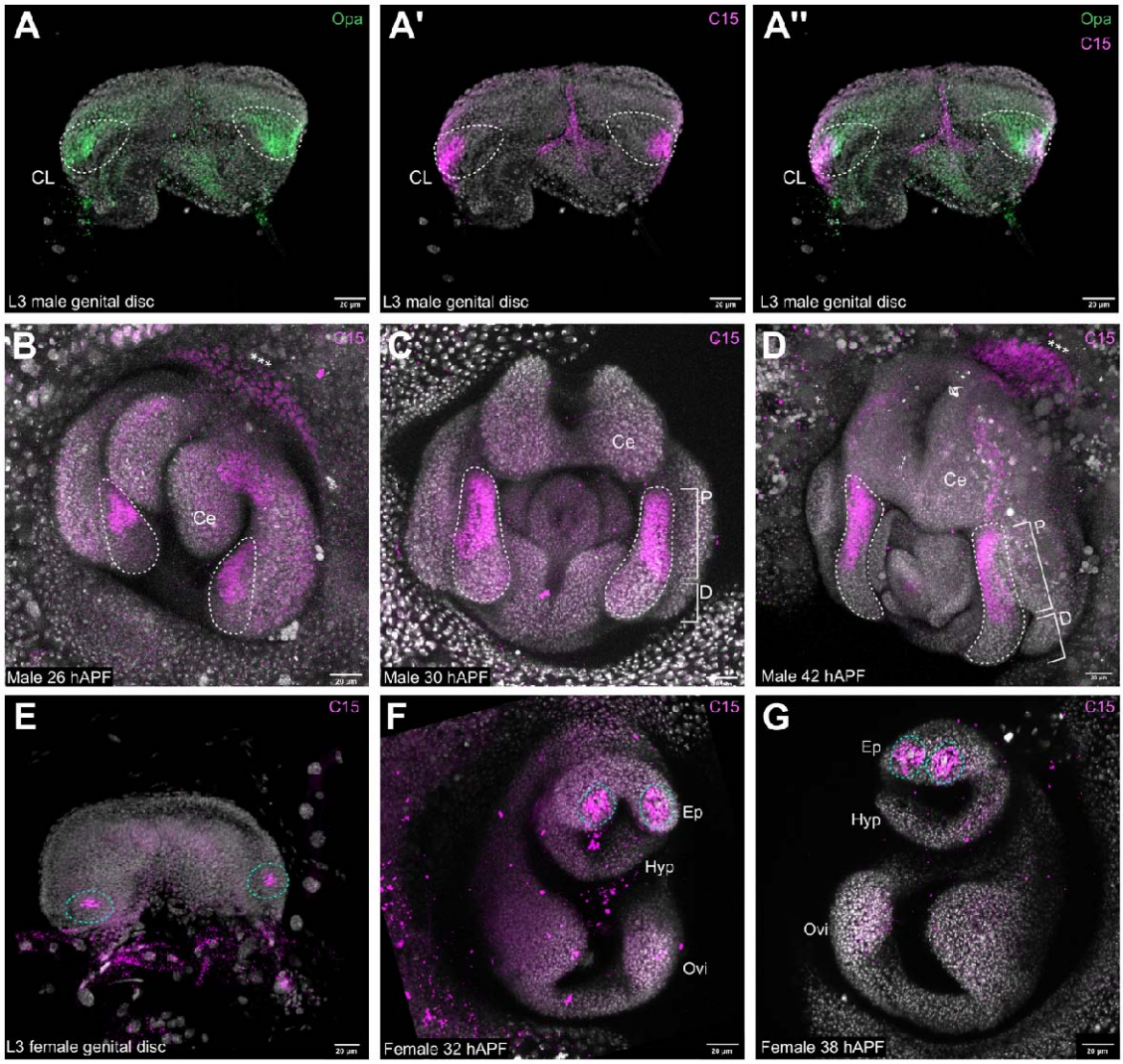

Figure 2. C15 expression in developing male and female terminalia. (A-A'') During male genital disc development, C15 is expressed at the clasper primordium (CL), as confirmed by overlap in expression with Opa. (B-D) During male terminalia pupal development, C15 is expressed in the proximal region of the clasper. C15 expression is also observed peripheral to the cerci (Ce) and at the adjoining terminal tissue (marked by ***). (E) C15 is expressed in a specific cluster of cells within the female cerci primordia. (F,G) During female terminalia pupal development, C15 is expressed in the epiproct (Ep), encircling two prominent bristle progenitor cells. White dashed outlines mark the developing male claspers. Cyan dashed outlines mark C15 expression in the female epiproct. Proximal (P) and distal (D) domains of the male pupal claspers are labelled in C and D. All genital discs are the ventral view. Hyp: Hypoproct, Ovi: Ovipositor. All samples were counterstained with DAPI.

C15 *is required for bristle development in male and female developing terminalia*

We then examined the role of *C15* during male and female terminalia development using RNAi knockdown. In males, we found that knockdown of *C15* expression resulted in a 17% increase in clasper bristle number (Fig. 3A; Supplementary Table 1). The extra ectopic bristles developed in the internal proximal domain of the clasper, a region that normally only displays bristles along the outer periphery (Fig. 3C-D') [58], consistent with C15 expression in this region (Fig. 2C). The Hox gene, *Abd-B*, is expressed in all structures of the male genitalia and dictates tissue identity (Supplementary Fig. 1A). RNAi against *Abd-B* appeared to only produce a weak knockdown

because the genitalia still developed relatively normally, but we did observe a significant decrease in clasper bristles (Supplementary Fig. 1B). Consistent with this, *Abd-B* RNAi knockdown appeared to extend C15 expression somewhat into the distal clasper domain, as well as generating stronger C15 expression surrounding the cerci (Supplementary Fig. 1C,D; Supplementary Table 1). Together, these results suggest that C15 represses clasper bristle development proximally and that this localisation of *C15* is regulated in part by Abd-B repression.

RNAi knockdown of *C15* also significantly increased the area of the male cerci (Fig. 3B) (Supplementary Table 1), although this gene is only expressed at the boundary of this structure (Fig. 2D). However, no difference in cerci bristle number was detected upon *C15* knockdown (Supplementary Fig. 2B). Surprisingly, male T2 tibia length also increased upon C15 knockdown even though this gene is not expressed in this part of the developing leg (Supplementary Fig. 2A).

In females, *C15* RNAi knockdown eliminated the two prominent epiproctal sensilla (Fig. 4A,A'), consistent with the expression of this transcription factor (Fig. 2F,G). The loss of female epiproct bristles contrasts with the gain of male clasper bristles upon *C15* RNAi knockdown (Fig. 3). However, *C15* RNAi knockdown in females had no significant effect on the total number of surrounding epiproct bristles compared to controls, although the area of the epiproct did significantly decrease (Fig. 4B,B'; Supplementary Table 2). *C15* RNAi knockdown had no detectable effect on the hypoproct or ovipositor bristle patterning, and unlike in males there was no significant effect on female tibia length (Supplementary Fig. 2D-G). In summary, these results revealed an epiproctal-specific role for *C15* in females, where it appears necessary for the development of the two prominent epiproctal sensilla and epiproctal size.

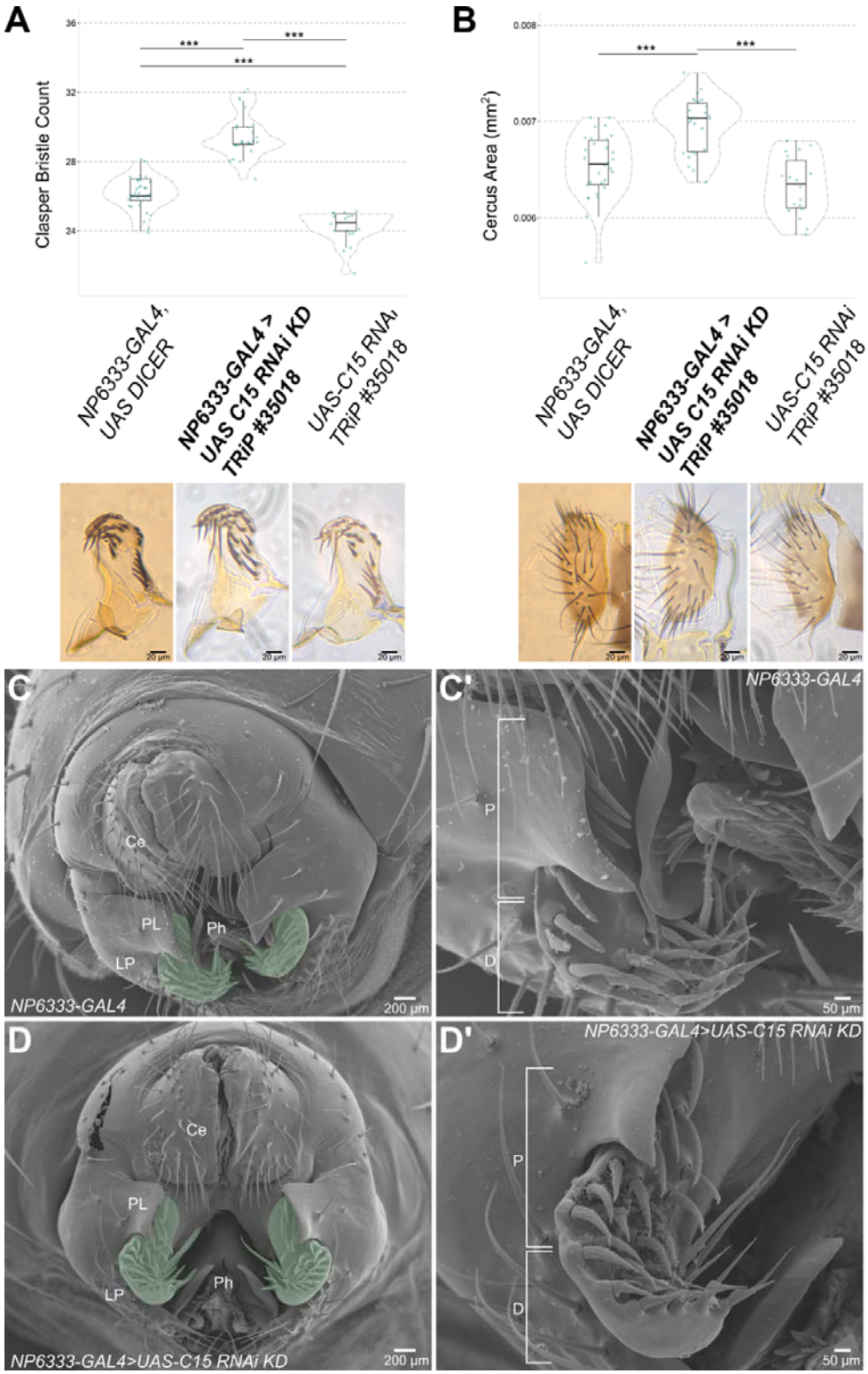

Figure 3. RNAi knockdown of *C15* during male terminalia development. (A) RNAi knockdown of *C15* in the developing male terminalia increased clasper bristle count, and (B) increased cercus size. SEM images of *NP6333-GAL4* parental control (C,C') and of *NP6333-GAL4>UAS-C15* RNAi knockdown (D,D'). *** $p < 0.001$, ($n > 17$) (Supplementary Table 1). (C, D) Green shading marks the claspers. (C',D') Proximal (P) and distal (D) regions of the clasper are indicated.

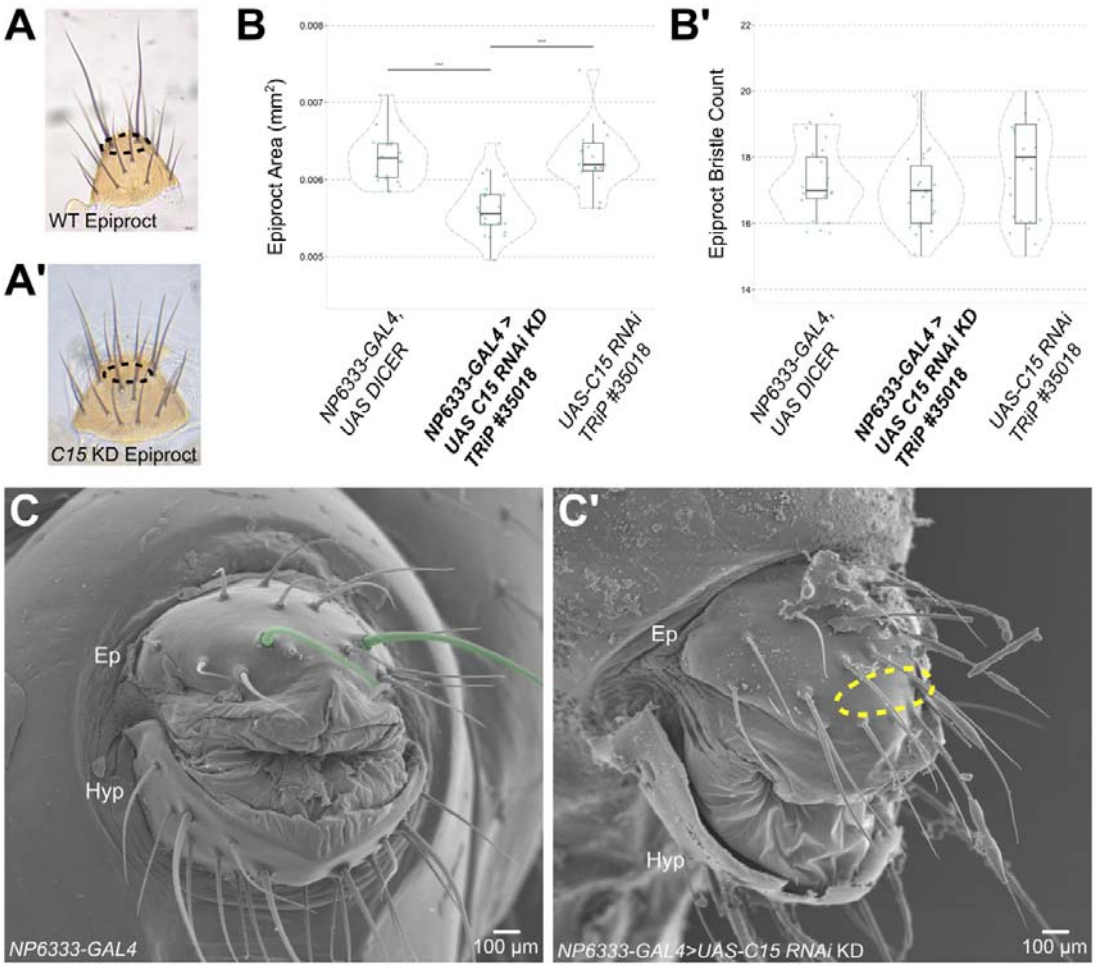

Figure 4. RNAi knockdown of *C15* during female terminalia development. (A,A') Light microscopy images of the female epiproct, where the dashed black ovals mark the region of the two prominent epiproctal sensilla. Scale bars are 20 µm. (B) RNAi knockdown of *C15* significantly reduced the epiproct area, but did not significantly affect the total epiproct bristle count (B'). *** $p < 0.001$, ($n > 17$) (Supplementary Table 2). (C) SEM image of *NP6333-GAL4* parental control. The two prominent epiproctal sensilla are coloured green. (C') *NP6333-GAL4>UAS-C15* RNAi knockdown female terminalia. The dashed yellow oval marks the loss of the two longer epiproctal sensilla. Ep: Epiproct and Hyp: Hypoproct.

Expression of dac, Dll and bab2 during male terminal development

C15 is a crucial component of the GRN underlying distal leg development [10, 11]. We have shown that this transcription factor also regulates the patterning of the male clasper and female epiproct. We next further investigated the expression and function of other key leg transcription factors in the male terminalia.

In the developing leg, *dac* is expressed proximally up to the first tarsal segment but is absent from the most distal tarsal segments and the pre-tarsal region [59] (Fig. 1B). It was previously shown that *dac* is also expressed in the clasper primordia of the male genital disc (Fig. 1B) [17]. We used a hypomorphic allele of *dac* with a GAL4 insertion crossed to *UAS-GFP* to assay *dac* expression in pupal genitalia [60]. We observed that *dac* expression predominantly localises to the distal clasper and lateral plates, with weaker expression in the proximal domain of

these structures (Supplementary Fig. 3A). Consistent with this, the claspers of the *dac* hypomorphic mutants exhibited loss of bristles in the distal domain of the clasper (Supplementary Fig. 3B; Supplementary Table 1). The remaining bristles appeared elongated, similar to that of the single long mechanosensory bristle present on wild-type claspers (Supplementary Fig. 3B). These findings suggest that *dac* promotes male clasper bristle development but may also regulate bristle morphology.

Dll is expressed throughout the distal leg segment primordia, but its direct activation of *bab2* is competitively blocked by C15 in the developing pre-tarsal region [12] (Supplementary Fig. 4A). In the male genital disc, *Dll* is expressed in the cerci and phallic primordia (Fig. 1B) [31], which is consistent with Dll expression during terminal pupal development (Supplementary Fig. 3C). We found that Dll was also expressed in both the proximal and distal regions of the claspers during pupal development (Supplementary Fig. 3C). RNAi knockdown of *Dll* resulted in a small but significant increase in clasper bristle number (Supplementary Fig. 3B), and reduced cerci size and bristle count, consistent with previous *Dll* mutant phenotypes (Supplementary Table 1) [31]. However, we did not detect any obvious effect of *Dll* RNAi knockdown on the expression of C15 (Supplementary Fig. 3D,E). Interestingly, *bab2* and C15 expression do not overlap in the male genital disc (Supplementary Fig. 4B), nor during pupal stages. During male pupal development, *bab2* is only expressed in the distal clasper (as well as the cerci), which suggests C15 may inhibit Dll-mediated activation of *bab2* in the proximal clasper like that seen in the pre-tarsal region of the leg (Supplementary Fig. 4B-C'') [12].

Al and Lim1 expression and function in the male and female terminalia

In leg imaginal discs, *C15* expression completely overlaps with *Lim1* and *al* in the leg pre-tarsal primordia, and their expression is maintained in this distal region throughout pupal leg development (Supplementary Fig. 5) [10, 11]. In the developing pre-tarsal region, these three transcription factors co-regulate one another, for example, loss of *C15* reduces *al* expression and vice versa, and loss of either *al* or *C15* abolishes *Lim1* expression. Furthermore, *C15* expression is markedly reduced in *Lim1* mutants. These positive regulatory interactions between these three transcription factors are essential for tarsal claw development [10, 11, 15].

We therefore assayed their relative expression during terminalia development. Unlike C15, we did not detect any Al expression in the developing male claspers during larval or pupal stages (Fig. 5A,A'). Consistent with this, RNAi knockdown of *al* showed no detectable clasper phenotype and did not affect C15 expression (Supplementary Fig. 6).

In the female genital disc, Al is not expressed in the epiproctal primordium marked by C15 (Fig. 5E). However, post-metamorphosis, Al is expressed ventral to the two prominent epiproctal sensilla in pupae (Fig. 5F,F'). Note that while it appears that Al and C15 are expressed in the same region of the epiproct, we were unable to determine the extent of their overlap because both antibodies originated from rat.

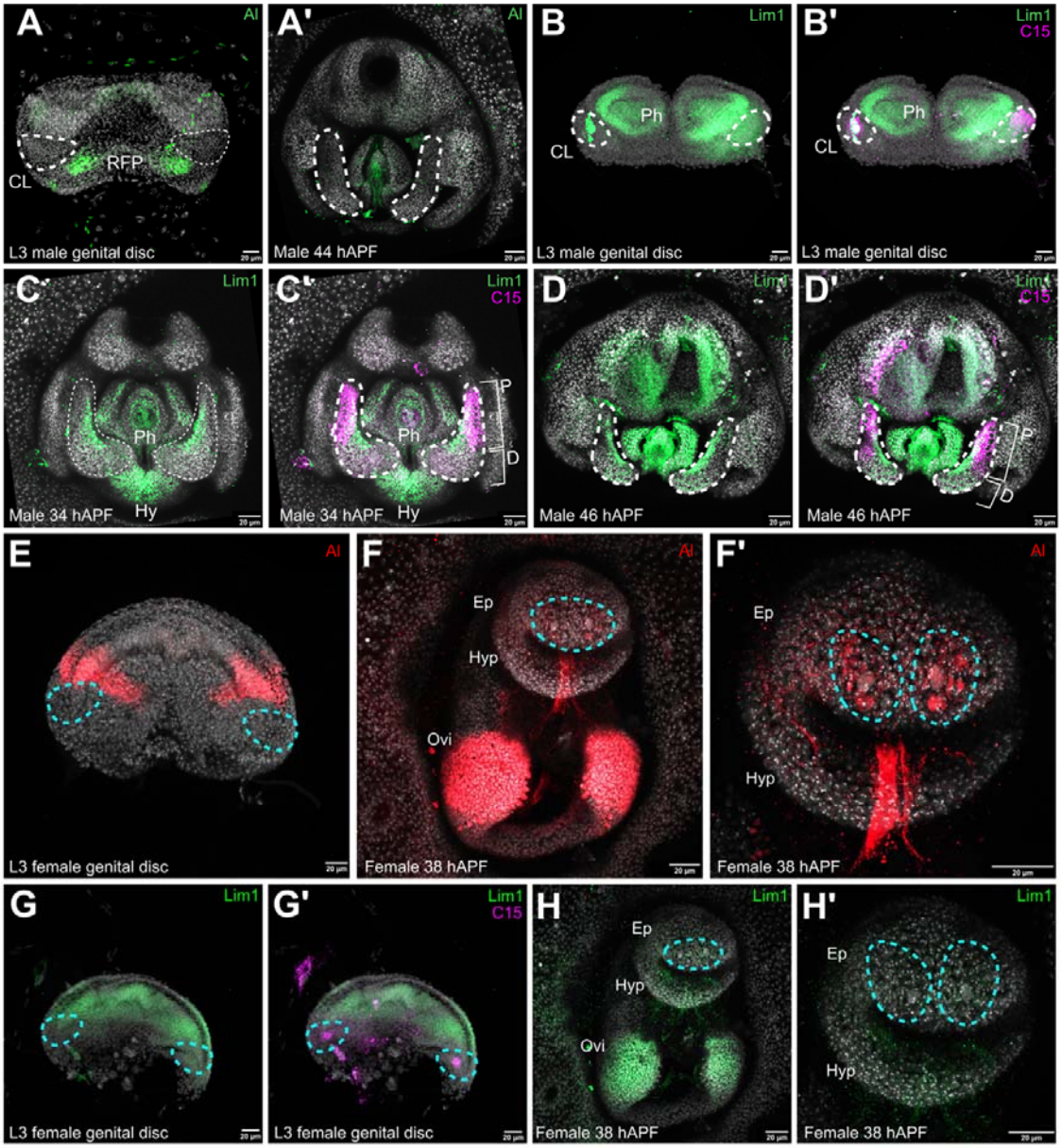

Figure 5. Expression of Al and Lim1 in the male and female developing terminalia. Al is expressed in the repressed female primordium (RFP) of the male genital disc but not in the primordia of any genital structures in the disc or during pupal stages (A,A'). (B,B') Lim1 is expressed in the phallic region (Ph) of the male genital disc, and partially overlaps with C15 expression in the clasper primordia (CL). (C-D') During male pupal development, Lim1 is expressed in the inner region of the proximal (P) and distal (D) clasper domains, where it partially overlaps with C15 proximally. Lim1 is also expressed throughout the phallic structures and hypandrium (Hy). (E) In female genital discs, Al is expressed in a defined region of the hypogynium [34]. (F) During female pupal development, Al is expressed in the female ovipositor (Ovi) and epiproct (Ep). (F') Al expression is ventral to the two prominent epiproctal sensilla. (G,G') Lim1 is expressed in the hypogynium primordium of the female genital disc, but does not overlap with C15 expression in the cerci primordia. (H,H') Lim1 is only expressed in the ovipositor of female pupal terminalia. Hyp: Hypoproct. (A-D') Dashed white outlines mark the clasper primordia. (E,H') Dashed cyan ovals mark the epiproctal C15 expression region. All samples were counterstained with DAPI.

RNAi knockdown of *al* decreased epiproct bristle count although the two prominent sensilla specified by C15 were still present (Fig. 6A). The epiproct area also decreased upon knockdown of *al* expression (Fig. 6A), consistent with its expression pattern (Fig. 5F,F'). Knockdown of *al* expression resulted in loss of C15 in the cells ventral to the epiproctal sensilla (Fig. 6C-D'), where they overlap in expression (Fig. 5). RNAi knockdown of *C15* also completely abolished Al expression in the epiproct (Fig. 6E-F'). Taken together these results confirm that there is positive regulation between *al* and *C15* in the female epiproct like that seen in the leg pre-tarsal region [10, 11, 13].

We observed Lim1 expression in male genital discs partially overlapping with C15 (Fig. 5G'). During pupal stages, Lim1 expression was maintained in the clasper and was also observed in the hypandrium and phallus (Fig. 5C-D'). At 34 hAPF, as the clasper and lateral plate primordia are separating, Lim1 is expressed in a thin strip of cells at the inner region of the clasper, partially overlapping with C15 in the proximal region and reflecting their earlier relative expression in the genital disc (Fig. 5C,C'). In older pupae, Lim1 clasper expression extends further distally retaining some overlap with C15 in the proximal domain (Fig. 5D,D').

Lim1 RNAi knockdown resulted in significantly fewer clasper bristles (Fig. 6B). These *Lim1* knockdown phenotypes are the opposite of what we saw with *C15* RNAi knockdown (Fig. 3). Furthermore, unlike in the developing pre-tarsal region, there does not appear to be an obvious regulatory interaction between C15 and Lim1 in male genitalia because although their expression overlaps in a few cells in the developing claspers, RNAi against one had no detectable effect on the other's expression pattern (Fig. 6G-N).

In developing female terminalia, there was no observable Lim1 protein localisation in the epiproct during larval and pupal development, although, unlike C15, Lim1 was expressed in the ovipositor (Fig. 5H). As expected, *Lim1* RNAi knockdown in females did not affect epiproct bristle or area compared to both parental controls (Supplementary Fig. 6B). However, *Lim1* RNAi knockdown did decrease ovipositor bristle number, consistent with its expression pattern (Supplementary Fig. 6C,C').

In summary, we have assayed the expression patterns and roles of the leg pre-tarsal core trio of transcription factors in both male and female developing terminalia. In males, only Lim1 and C15 regulate clasper development, whereas in females, only C15 and Al regulate epiproct bristle patterning. These results contrast with the leg and aristae, which both employ all three of these transcription factors.

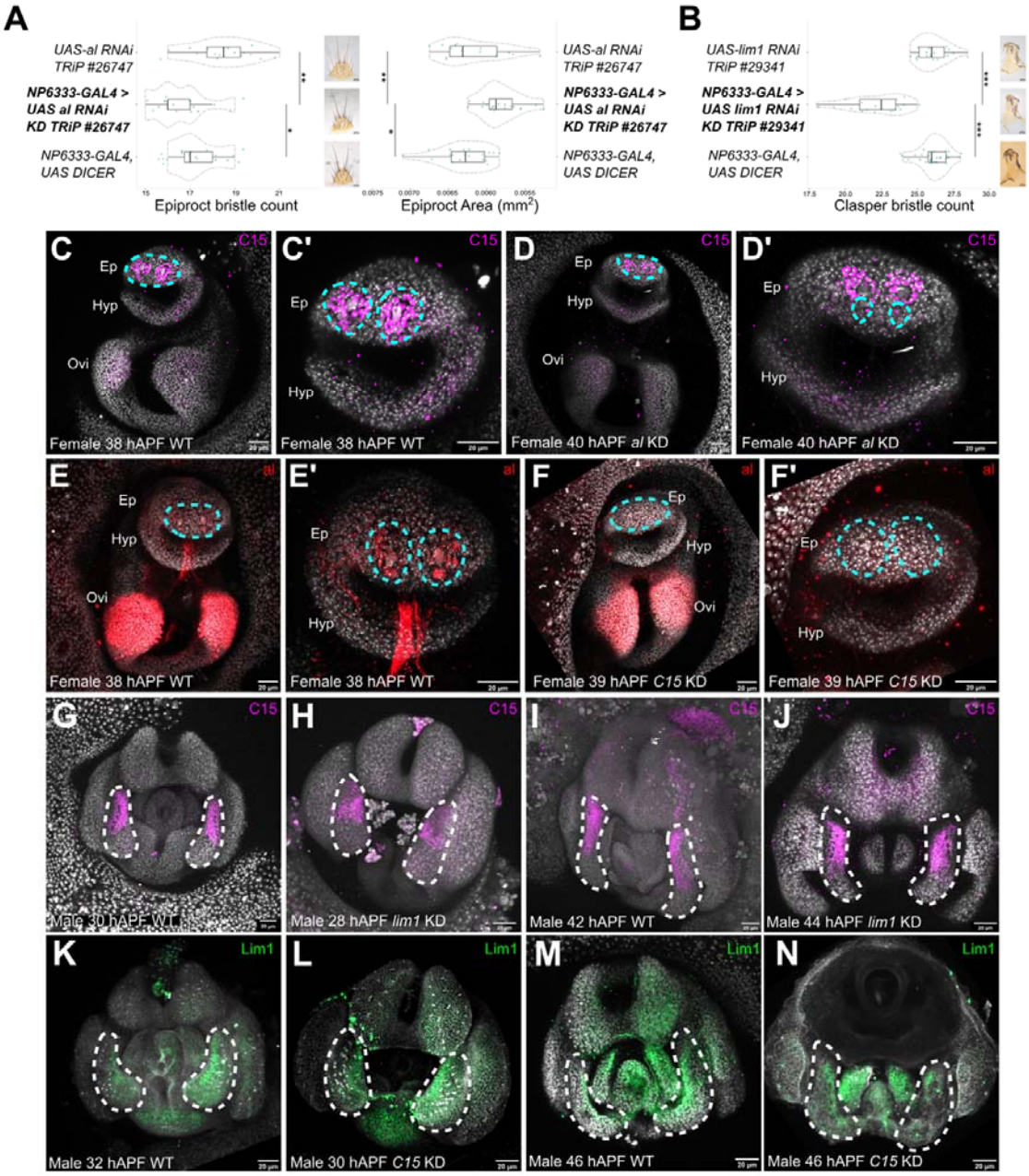

Figure 6. Roles of *Lim1* and *al* during male and female terminalia development respectively. (A) In females, *al* RNAi knockdown reduced epiproct bristle count, and area. (B) In males, *Lim1* RNAi knockdown significantly reduced clasper bristle count. *** $p < 0.001$, ** $p < 0.01$, * $p < 0.05$ (Supplementary Tables 1 and 2). $n > 14$ for all lines phenotyped. (C,C') Wild type (WT) C15 expression in the female pupal epiproct. (D,D') *al* RNAi knockdown abolished C15 expression only in cells ventral to the female epiproctal sensilla primordia. (E,E') WT C15 expression at the female pupal ovipositor and epiproct. (F,F') *C15* RNAi knockdown entirely abolished Al expression in the female epiproct. (G,I) WT C15 expression in the proximal clasper domain in developing male terminalia. (H,J) *Lim1* RNAi knockdown did not appear to affect C15 expression in male pupal terminalia. (K,M) Lim1 expression in the inner region of the clasper, spanning both the proximal and distal regions. (L,N) *C15* RNAi knockdown did not appear to affect Lim1 expression in male pupal terminalia. Ep: Epiproct, Hyp: Hypoproct, Ovi: Ovipositor. (C-F') Dashed cyan ovals mark epiproctal C15 expression (apart from (F'), where it marks the loss of C15 expression). (G-N) Dashed white outlines mark the clasper primordia. All samples have been stained with DAPI.

A C15 *genital enhancer is not active in the developing leg or arista*

We next explored the cis-regulatory sequences that drive *C15* expression in the genitalia. Three GAL4 reporter lines spanning the first and second *C15* introns were available for this region (Fig. 7A) [47]. We then generated ATAC-seq data for male pupal genitalia to compare the profiles of the *C15* locus, and in particular the regions captured in reporter lines, with T2 pupal legs and L3 eye-antennal discs (Fig. 7A). The intron 1 region spanned relatively inaccessible chromatin in the genital, leg, and eye profiles (Fig. 7A). The Intron 2 enhancer 1 region contained two peaks in the genital track that were also accessible in profiles from the other two tissues (Fig. 7A). The intron 2 enhancer 2 region, which overlaps with intron 2 enhancer 1 by 1007 bp, and encompasses the previously mapped embryonic enhancer of *C15* [61] (Fig. 7A), is relatively inaccessible in all three tissues.

To assay the activity of the reporter lines, we crossed them to *UAS-GFP* and examined GFP signal in live pupae and fixed discs and pupal tissues (Fig. 7; Supplementary Fig. 7). The *C15* intron 1 region did not drive expression in leg or genital pupal structures as predicted from the lack of accessibility observed in the ATAC-seq profiles (Fig. 7A; Supplementary Fig. 7A,A'). However, this region was active in 3 or 4 leg disc cells some of which also expressed C15 (Supplementary Fig. 7C,C'). Female genital discs had no observable intron 1 enhancer activity, whereas the male genital disc did show reporter expression but in the repressed female primordium, which does not recapitulate endogenous *C15* expression (Supplementary Fig. 7).

Intron 2 enhancer 1 was active in the male terminalia but did not drive any specific expression in the female counterpart (Fig. 7B-C'). We detected intron 2 enhancer 1 activity in the clasper primordia of male genital discs, which was sustained during late pupal development (Fig. 7E-F''). This enhancer's activity recapitulated the endogenous expression of *C15* in the proximal clasper but this region was also able to drive expression in the distal clasper where *C15* is not expressed (Fig. 7F''). Intron 2 enhancer 1 was not active in leg discs nor the arista primordia of the antennal disc but was able to drive some expression in the ocellar primordium of the eye disc and notum in the wing disc (Fig. 7).

Intron 2 enhancer 2 lacked activity in leg and genital tissues (Supplementary Fig. 7F-G'). However, this enhancer was active in the notum of the wing which overlapped with endogenous C15 expression (Supplementary Fig. 7H) [62].

In summary, *C15* expression in the male genitalia is regulated, in part, by the intron 2 enhancer 1 region. Although this region also recapitulates aspects of the *C15* in the eye and wing discs, it does not drive expression in either the pre-tarsal region or arista primordia where *C15* overlaps with both *Lim1* and *al*.

We next used ATAC-seq footprinting to predict transcription factor binding sites in the intron 2 enhancer 1 region in the developing genitalia (Supplementary Tables 4 and 5). This analysis predicted high probability binding sites for Abd-B as well as other transcription factors expressed in the genitalia and analia, such as Daughterless and Cad [33], which could be candidates for

activation or repression of *C15* expression in these developing tissues, respectively (Supplementary Tables 4 and 5). Curiously, high probability binding sites were also detected for Al, but these may represent motifs bound by other homeobox-containing transcription factors because we found that Al is not expressed in developing male terminalia (Supplementary Tables 4 and 5).

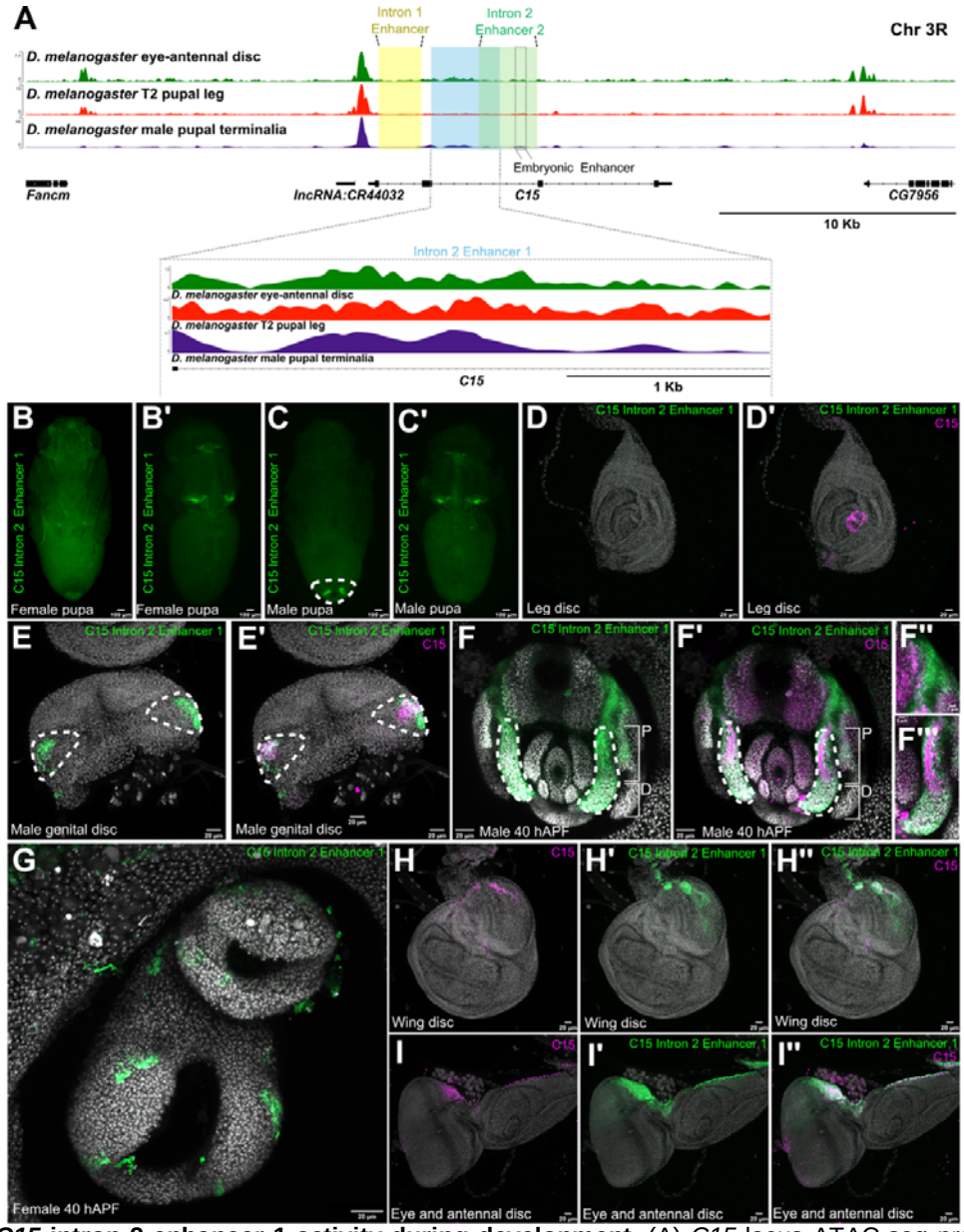

Figure 7. *C15* intron 2 enhancer 1 activity during development. (A) *C15* locus ATAC-seq profiles in T2 pupal legs, eye-antennal discs, and male pupal terminalia. Regions encompassed by genitalia enhancer reporter lines are labelled accordingly. (B-C') Image of *C15* intron 2 enhancer 1 driving *UAS-GFP* expression in live female (B,B') and male (C,C') late pupae. (B) In female pupae, C15 intron 2 enhancer 1 is not active in the ventral (B') but drives expression in the wing hinges and near the ocelli in the dorsal. (C) *C15* intron 2 enhancer 1 is active at the male pupal terminalia (encircled by a dashed oval), (C'), and in the wing hinges and near the ocelli in the dorsal view. (D,D') *C15* intron 2 enhancer 1 is not active in the leg disc. (E,E') *C15* intron 2 enhancer 1 is active in male genital discs and overlaps with endogenous C15 expression in the clasper primordia. (F-F''') This enhancer is active in the claspers and periphery of the cerci in male pupal terminalia and overlaps with C15 expression in the proximal region of the clasper. (G) *C15* intron 2 enhancer 1 does not drive any specific expression resembling endogenous C15 expression in developing female terminalia. (H-H'') This enhancer is active in the notum of the wing disc and overlaps with C15 expression. (I-I'') *C15* intron 2 enhancer 1 is active in the cuticle and ocelli primordium of eye-antennal discs and

overlapped with C15 expression. All samples have been stained with DAPI. P: proximal and D: distal clasper regions.

Discussion

C15 *regulates bristle patterning on the female epiproct and male claspers*

It was shown previously that C15 is vital for the development of the pre-tarsal claws, as well as the arista, ocellar postvertical bristles, and medial thorax bristles [10, 11]. *C15* is also expressed in the developing male genitalia and female analia [33] (this work) and we have shown that this transcription factor regulates bristle patterning on the male claspers and female epiproct. In females, C15 is required for the development of the two distinctive longer epiproct bristles consistent with the role of this transcription factor in promoting bristle development on other structures [10, 11]. The long epiproct bristles that require *C15* presumably play a role in copulation, but this has not been tested to the best of our knowledge. In contrast to promoting the development of female epiproct bristles, *C15* RNAi knockdown increased the number of male clasper bristles, indicating that C15 acts to repress bristle formation on these genital organs. These results suggest that C15 can play different roles in different developmental contexts that likely depend on which other transcription factors and co-factors it is expressed with in local GRNs.

C15 *GRN differences between male and female terminalia and among serially homologous appendages*

C15, Lim1 and Al overlap in expression in the aristae of the antennae and pre-tarsal region of the legs and are crucial for the correct development of these structures [10, 11, 14, 15]. However, we did not identify any male or female anal or genital structures where the expression of all three of these transcription factors overlapped. For example, we did not detect any Al expression in developing male claspers and only observed a small overlap in C15 and Lim1 expression in this developing organ (Fig. 8). Furthermore, our results suggest there is no regulatory interaction between Lim1 and C15 in the developing male claspers, and that they appear to play opposing roles in promoting and suppressing clasper bristle development, respectively.

In the developing female genitalia, in the ovipositor primordia, we found an overlap between Lim1 and Al expression but no C15 expression. We did not observe expression of any of these transcription factors in the male analia, but C15 is required for Al expression in the female epiproct, although Lim1 is not expressed in this tissue. Therefore, the expression, roles, and interactions of C15, Lim1, and Al differ between male and female terminal structures. These results are consistent with other tissues that employ these factors individually or in pairs [10, 11, 14, 15, 61]. Indeed, even in the pre-tarsus, for example, while Al and C15 combine to repress *Bar,* C15 is able to inhibit activation of *bab2* by Dll independently of Al, showing that even though their expression overlaps they can have different roles [10-13].

Our results show that although the legs and genitalia are thought to be serial homologs, the deployment of C15-Al-Lim1 has diverged between these development contexts. Nevertheless, we did detect similarities in C15 expression and potential regulatory interactions with other factors between the claspers and the pre-tarsal region consistent with their ancient serial homology. In the developing leg, *dac* is not expressed in the distal tarsal segments nor the pre-tarsal region where C15 is expressed, while *Dll* is expressed throughout the distal leg [9] (Fig. 8). In the clasper, *dac* is only expressed in the distal region where there is no C15 expression while *Dll* is expressed throughout the developing clasper (Fig. 8). Intriguingly, *bab2* is expressed in the distal clasper which suggests that Dll activates this gene in this domain but *bab2* expression is blocked by C15 in the proximal clasper perhaps by inhibition of Dll activation like in the pre-tarsal region of the leg [12] (Fig. 8). This is also consistent with the relative expression of C15 and another gene *tartan* (*trn*), which encodes a leucine-rich repeat transmembrane protein involved in boundary formation that positively regulates clasper size and bristle number [63, 64]. In the leg disc, Trn encircles pretarsal C15 expression, and *C15* RNAi knockdown in the leg significantly disrupted the accumulation of the Trn and the Tenascin-Major interacting scaffold protein, Par-3 [65], suggesting that C15 regulates their expression. In the clasper, Trn expression is mostly excluded from the C15 expression domain in the proximal clasper but Trn is expressed in the distal region of the clasper [63, 64]. This suggests C15 may repress *trn* expression in both the developing leg and developing male genitalia.

Taken together, the relative expression and functions of *C15* and other genes suggest that *C15* patterns the proximal region of the clasper in a similar way to its role in the pre-tarsal region, but that there are key differences in wiring of the GRNs in these serial homologs (Fig. 8).

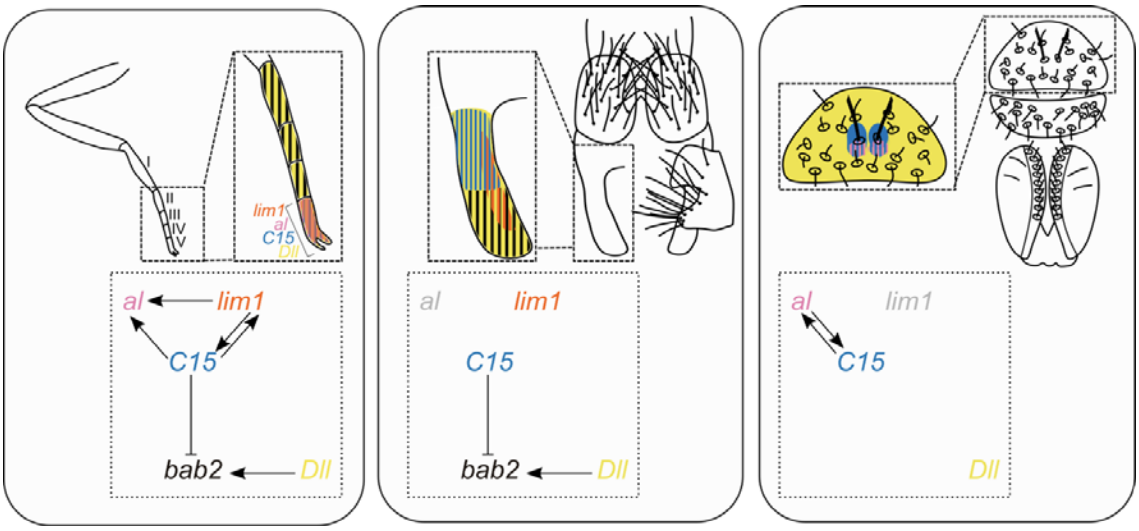

Figure 8. **Rewiring of the pretarsal leg GRN in the male claspers and female epiproct.**
Development of the pre-tarsal and tarsal segments is coordinated by a *C15*-centered GRN. *Lim1*, *al*, *bab2*, *Dll* and *C15* are expressed at the distal region of the leg where the claw protrudes from. *C15* and *bab2* expression are mutually exclusive to tarsal segments II-IV and the pretarsal region, respectively, while *Dll* spans the entire tarsus. *C15*, *Lim1* and *al* are all expressed in the pretarsal region and wired into an interdependent positive feedback loop. The entire male claspers and female epiproct are marked by *Dll*

expression, like the tarsal segments of the leg. Similar to the leg, *C15* and *bab2* are expressed in mutually exclusive regions of the proximal and distal clasper, respectively. *Lim1* expression spans a thin inner strip of cells bridging the proximal and distal regions of the clasper. *al* is not expressed in the clasper. The female epiproct lacks *Lim1* expression. However, like the pretarsal region of the leg, *al* and *C15* show overlapping expression patterns. *bab2* expression in the female epiproct was not assayed in this study. Data summarised from this work and previous studies [9, 17, 31, 35, 36].

Regulation of C15 *expression in developing terminalia*

We identified an enhancer that recapitulates *C15* expression in the developing male genitalia, although the activity of this cis-regulatory element extends into the distal region of the pupal clasper, where this transcription factor is not expressed. This ectopic activity somewhat resembles the expansion of C15 expression we observed upon *Abd-B* RNAi, which suggests that although we detected binding sites for this Hox factor in the *C15* enhancer, additional Abd-B sites may be needed to repress *C15* in the distal clasper. Other possible candidate transcription factors that may directly activate this enhancer inferred from ATAC-seq footprinting include Da and Cad, which could activate and repress *C15* in the male genitalia and analia respectively [33]. However, some of the most highly sites significant sites identified by JASPER and CIS-BP were for predicted homeobox binding targets and given these transcription factors can bind very similar motifs, further work is needed to identify which transcription factors directly regulate *C15* (Supplementary Tables 4 and 5). The *C15* genital enhancer we have identified also drives expression consistent with endogenous *C15* expression in the ocelli primordia of the eye-antennal disc and notum of the wing disc, but again, additional analysis is needed to identify the transcription factor binding sites responsible for the regulation of this element in these tissues and whether some of the same motifs are used in the genitalia or not.

Our results suggest that *C15* employs a different enhancer in developing female terminalia since the enhancer we identified does not drive expression of a *C15* pattern in the epiproct. It is also clear from our results that the previously characterised 650 bp embryonic *C15* enhancer (within the intron 2 enhancer 2 region), which is directly regulated by Zen and Smad [61], does not drive expression in either male or female terminalia, although this region may be active in the wing notum.

None of the putative *C15* enhancer fragments we tested, including the identified genital enhancer, recapitulated endogenous *C15* expression in the leg disc, although the intron 1 enhancer was active in a few cells in the centre of the disc suggesting it may contain binding sites that contribute to C15 expression in the pre-tarsal region. These results imply that even though *C15* is expressed in these serial homologues it is regulated by distinct enhancer elements. This modularity may underpin tissue-specific regulatory logic, presumably programmed by different Hox inputs such as Abd-B in the genitalia, and that could have contributed to the diversification of these serially homologous structures from the ‘ground state’ ventral appendage [16]. It would be very interesting to identify the *C15* pre-tarsal and arista enhancers to compare to the genital enhancer that we have identified to understand the differences in *C15* regulation and the GRNs in these

developing tissues better. Interestingly, a previous study of bristle number evolution between *D. yakuba* and *D. santomea*, found that the same cis-regulatory change in one enhancer of the *scute* gene affected both sex comb teeth number and hypandrial bristle number in male forelegs and genitalia, respectively [66]. Therefore, changes in a single pleiotropic enhancer can also contribute to changes in the morphology of different secondary sexual structures.

Divergence in male genitalia among Drosophila species

Male terminal structures show great diversity in shape, size and bristle composition, but there are also differences among female structures [67, 68]. Given the role of *C15* in bristle patterning in male and female terminalia, this gene represents an excellent candidate for differences in the terminal bristle patterns among species.

It has been shown that the male clasper bristles intercalate with the bristles of the female oviscapt during copulation and therefore it is likely that the correct pattern of bristles regulated by *C15* is important for mating [69]. *D. mauritiana* has more clasper bristles than its sibling species *D. simulans* and *D. melanogaster*, and we previously showed that *trn* contributes to this difference [63, 64, 70]. Given that C15 may regulate *trn* expression in the developing claspers and that *C15* is also located in a mapped region shown to contribute to the clasper bristle number difference between *D. simulans* and *D. mauritiana* [64, 70], this gene, and in particular the enhancer we have identified that is active in the developing claspers, represents an excellent candidate for contributing to this evolutionary difference in genital morphology. Furthermore, *D. teissieri* claspers are covered in bristles, including much of the proximal clasper domain that is naked in the *D. melanogaster* subgroup and marked by C15 expression [71, 72]. It would therefore be very interesting to explore *C15* expression and function in *D. teissieri* to see whether the bristles in the proximal clasper domain result from the loss of *C15* expression and if this reflects any changes in the activity of the *C15* clasper enhancer we have identified.

Conclusions

We have shown that *C15* is required for the patterning of the bristles in male and female terminal structures. This involves similarities and differences to the regulatory interactions of this transcription factor in other serially homologous appendages, and in particular, the C15-Lim1-Al trio is not used in either male or female terminal, unlike the antennal aristae and leg pre-tarsal region. Furthermore, *C15* expression appears to be regulated by a different enhancer in the developing male genitalia compared to legs and antennae, which likely unpins the different regulatory logic used in these serially homologues and this modularity may even have facilitated a role for *C15* in the rapid diversification of male genitalia.

Acknowledgments

This study was funded in part by a BBSRC (BB/X006689/1) grant to A.P.M. and M.D.S.N., a BBSRC DTP studentship (BB/ M011224/1) to A.M.R. We thank the Bloomington *Drosophila* Stock Center and Vienna *Drosophila* RNAi Center for fly lines. Microscopy and imaging was carried out in the Centre for Bioimaging at Oxford Brookes University. We thank Gerard Campbell for generously providing antibodies.

Author contributions

The project was conceived by A.M.R., A.P.M. and M.D.S.N. Experiments were carried out by A.M.R. and J.F.J. Data were analysed by all authors. A.M.R and A.P.M. wrote the paper, assisted by M.D.S.N. and J.F.J.

Declaration of interests

The authors declare they have no competing interests**.**

References

1. Carroll SB, Grenier JK, Weatherbee SD. From DNA to diversity : molecular genetics and the evolution of animal design. 2nd ed. Malden, MA: Blackwell Pub.; 2005.
2. Jockusch EL, Williams TA, Nagy LM. The evolution of patterning of serially homologous appendages in insects. Dev Genes Evol. 2004;214(7):324-38. Epub 20040529. doi: 10.1007/s00427-004-0412-6.
3. Jockusch EL. Developmental and Evolutionary Perspectives on the Origin and Diversification of Arthropod Appendages. Integr Comp Biol. 2017;57(3):533-45. doi: 10.1093/icb/icx063.
4. Pechmann M, Khadjeh S, Sprenger F, Prpic NM. Patterning mechanisms and morphological diversity of spider appendages and their importance for spider evolution. Arthropod Struct Dev. 2010;39(6):453-67. doi: 10.1016/j.asd.2010.07.007.
5. Browne WE, Patel NH. Molecular genetics of crustacean feeding appendage development and diversification. Semin Cell Dev Biol. 2000;11(6):427-35. doi: 10.1006/scdb.2000.0196.
6. Williams TA, Nagy LM. Developmental modularity and the evolutionary diversification of arthropod limbs. J Exp Zool. 2001;291(3):241-57. doi: 10.1002/jez.1101.
7. Khan S, Dilsha C, Shashidhara LS. Haltere development in D. melanogaster: implications for the evolution of appendage size, shape and function. Int J Dev Biol. 2020;64(1-2-3):159-65. doi: 10.1387/ijdb.190133LS.
8. Ando T, Fujiwara H, Kojima T. The pivotal role of aristaless in development and evolution of diverse antennal morphologies in moths and butterflies. BMC Evol Biol. 2018;18(1):8. Epub 20180125. doi: 10.1186/s12862-018-1124-2.
9. Ruiz-Losada M, Blom-Dahl D, Cordoba S, Estella C. Specification and Patterning of Drosophila Appendages. J Dev Biol. 2018;6(3). Epub 20180714. doi: 10.3390/jdb6030017.
10. Campbell G. Regulation of gene expression in the distal region of the Drosophila leg by the Hox11 homolog, C15. Dev Biol. 2005;278(2):607-18. doi: 10.1016/j.ydbio.2004.12.009.
11. Kojima T, Tsuji T, Saigo K. A concerted action of a paired-type homeobox gene, aristaless, and a homolog of Hox11/tlx homeobox gene, clawless, is essential for the distal tip development of the Drosophila leg. Dev Biol. 2005;279(2):434-45. doi: 10.1016/j.ydbio.2004.12.005.
12. Mojica-Vazquez LH, Benetah MH, Baanannou A, Bernat-Fabre S, Deplancke B, Cribbs DL, et al. Tissue-specific enhancer repression through molecular integration of cell signaling inputs. PLoS Genet. 2017;13(4):e1006718. Epub 20170410. doi: 10.1371/journal.pgen.1006718.

13. Miyazono K, Zhi Y, Takamura Y, Nagata K, Saigo K, Kojima T, et al. Cooperative DNA-binding and sequence-recognition mechanism of aristaless and clawless. EMBO J. 2010;29(9):1613-23. Epub 20100413. doi: 10.1038/emboj.2010.53.
14. Schneitz K, Spielmann P, Noll M. Molecular genetics of aristaless, a prd-type homeo box gene involved in the morphogenesis of proximal and distal pattern elements in a subset of appendages in Drosophila. Genes Dev. 1993;7(1):114-29. doi: 10.1101/gad.7.1.114.
15. Tsuji T, Sato A, Hiratani I, Taira M, Saigo K, Kojima T. Requirements of Lim1, a Drosophila LIM-homeobox gene, for normal leg and antennal development. Development. 2000;127(20):4315-23. doi: 10.1242/dev.127.20.4315.
16. Casares F, Mann RS. The ground state of the ventral appendage in Drosophila. Science. 2001;293(5534):1477-80. doi: 10.1126/science.1062542.
17. Estrada B, Sanchez-Herrero E. The Hox gene Abdominal-B antagonizes appendage development in the genital disc of Drosophila. Development. 2001;128(3):331-9. doi: 10.1242/dev.128.3.331.
18. Stansbury MS, Moczek AP. The function of Hox and appendage-patterning genes in the development of an evolutionary novelty, the Photuris firefly lantern. Proc Biol Sci. 2014;281(1782):20133333. Epub 20140319. doi: 10.1098/rspb.2013.3333.
19. Stern DL. The Hox gene Ultrabithorax modulates the shape and size of the third leg of Drosophila by influencing diverse mechanisms. Dev Biol. 2003;256(2):355-66. doi: 10.1016/s0012-1606(03)00035-6.
20. Buffry AD, Kittelmann S, McGregor AP. Characterisation of the role and regulation of Ultrabithorax in sculpting fine-scale leg morphology. Front Cell Dev Biol. 2023;11:1119221. Epub 20230213. doi: 10.3389/fcell.2023.1119221.
21. Kittelmann S, Buffry AD, Franke FA, Almudi I, Yoth M, Sabaris G, et al. Gene regulatory network architecture in different developmental contexts influences the genetic basis of morphological evolution. PLoS Genet. 2018;14(5):e1007375. Epub 20180503. doi: 10.1371/journal.pgen.1007375.
22. Buffry AD, McGregor AP. Micromanagement of Drosophila Post-Embryonic Development by Hox Genes. J Dev Biol. 2022;10(1). Epub 20220218. doi: 10.3390/jdb10010013.
23. Delker RK, Ranade V, Loker R, Voutev R, Mann RS. Low affinity binding sites in an activating CRM mediate negative autoregulation of the Drosophila Hox gene Ultrabithorax. PLoS Genet. 2019;15(10):e1008444. Epub 20191007. doi: 10.1371/journal.pgen.1008444.
24. Diaz-de-la-Loza MD, Loker R, Mann RS, Thompson BJ. Control of tissue morphogenesis by the HOX gene Ultrabithorax. Development. 2020;147(5). Epub 20200302. doi: 10.1242/dev.184564.
25. Pavlopoulos A, Akam M. Hox gene Ultrabithorax regulates distinct sets of target genes at successive stages of Drosophila haltere morphogenesis. Proc Natl Acad Sci U S A. 2011;108(7):2855-60. Epub 20110131. doi: 10.1073/pnas.1015077108.
26. Paul R, Giraud G, Domsch K, Duffraisse M, Marmigère F, Khan S, et al. Hox dosage contributes to flight appendage morphology in Drosophila. Nat Commun. 2021;12(1):2892. Epub 20210517. doi: 10.1038/s41467-021-23293-8.
27. Eksi SE, Barmina O, McCallough CL, Kopp A, Orenic TV. A Distalless-responsive enhancer of the Hox gene Sex combs reduced is required for segment- and sex-specific sensory organ development in Drosophila. PLoS Genet. 2018;14(4):e1007320. Epub 20180410. doi: 10.1371/journal.pgen.1007320.
28. Estrada B, Casares F, Sanchez-Herrero E. Development of the genitalia in Drosophila melanogaster. Differentiation. 2003;71(6):299-310. doi: 10.1046/j.1432-0436.2003.03017.x.
29. McQueen EW, Afkhami M, Atallah J, Belote JM, Gompel N, Heifetz Y, et al. A standardized nomenclature and atlas of the female terminalia of Drosophila melanogaster. Fly (Austin). 2022;16(1):128-51. doi: 10.1080/19336934.2022.2058309.
30. Rice G, David JR, Kamimura Y, Masly JP, McGregor AP, Nagy O, et al. A standardized nomenclature and atlas of the male terminalia of Drosophila melanogaster. Fly (Austin). 2019;13(1-4):51-64. Epub 20190819. doi: 10.1080/19336934.2019.1653733.
31. Gorfinkiel N, Sanchez L, Guerrero I. Drosophila terminalia as an appendage-like structure. Mech Dev. 1999;86(1-2):113-23. doi: 10.1016/s0925-4773(99)00122-7.

32. Sanchez L, Casares F, Gorfinkiel N, Guerrero I. The genital disc of Drosophila melanogaster : II. Role of the genes hedgehog, decapentaplegic and wingless. Dev Genes Evol. 1997;207(4):229-41. doi: 10.1007/s004270050111.
33. Vincent BJ, Rice GR, Wong GM, Glassford WJ, Downs KI, Shastay JL, et al. An Atlas of Transcription Factors Expressed in Male Pupal Terminalia of Drosophila melanogaster. G3 (Bethesda). 2019;9(12):3961-72. Epub 20191203. doi: 10.1534/g3.119.400788.
34. Chatterjee SS, Uppendahl LD, Chowdhury MA, Ip P-L, Siegal ML. The female-specific Doublesex isoform regulates pleiotropic transcription factors to pattern genital development in Drosophila. Development. 2011;138(6):1099-109. doi: 10.1242/dev.055731.
35. Keisman EL, Baker BS. The Drosophila sex determination hierarchy modulates wingless and decapentaplegic signaling to deploy dachshund sex-specifically in the genital imaginal disc. Development. 2001;128(9):1643-56. doi: 10.1242/dev.128.9.1643.
36. Gorfinkiel N, Sanchez L, Guerrero I. Development of the Drosophila genital disc requires interactions between its segmental primordia. Development. 2003;130(2):295-305. doi: 10.1242/dev.00214.
37. Dietzl G, Chen D, Schnorrer F, Su KC, Barinova Y, Fellner M, et al. A genome-wide transgenic RNAi library for conditional gene inactivation in Drosophila. Nature. 2007;448(7150):151-6. doi: 10.1038/nature05954.
38. Stieper BC, Kupershtok M, Driscoll MV, Shingleton AW. Imaginal discs regulate developmental timing in Drosophila melanogaster. Dev Biol. 2008;321(1):18-26. Epub 20080609. doi: 10.1016/j.ydbio.2008.05.556.
39. Stern D, Sucena E. Preparation of larval and adult cuticles for light microscopy. Drosophila protocols. 2000:601-15.
40. Schneider CA, Rasband WS, Eliceiri KW. NIH Image to ImageJ: 25 years of image analysis. Nat Methods. 2012;9(7):671-5. doi: 10.1038/nmeth.2089.
41. Hackett JL, Wang X, Smith BR, Macdonald SJ. Mapping QTL Contributing to Variation in Posterior Lobe Morphology between Strains of Drosophila melanogaster. PLoS One. 2016;11(9):e0162573. Epub 20160908. doi: 10.1371/journal.pone.0162573.
42. R Core Team. R: A language and environment for statistical computing. Vienna, Austria: R Foundation for Statistical Computing; 2020.
43. Hothorn T, Bretz F, Westfall P. Simultaneous inference in general parametric models. Biom J. 2008;50(3):346-63. doi: 10.1002/bimj.200810425.
44. Benjamini Y, Hochberg Y. Controlling the False Discovery Rate: A Practical and Powerful Approach to Multiple Testing. Journal of the Royal Statistical Society: Series B (Methodological). 1995;57(1):289-300. doi: https://doi.org/10.1111/j.2517-6161.1995.tb02031.x.
45. Bainbridge SP, Bownes M. Staging the metamorphosis of Drosophila melanogaster. J Embryol Exp Morphol. 1981;66:57-80.
46. Schindelin J, Arganda-Carreras I, Frise E, Kaynig V, Longair M, Pietzsch T, et al. Fiji: an open-source platform for biological-image analysis. Nat Methods. 2012;9(7):676-82. Epub 20120628. doi: 10.1038/nmeth.2019.
47. Jenett A, Rubin GM, Ngo TT, Shepherd D, Murphy C, Dionne H, et al. A GAL4-driver line resource for Drosophila neurobiology. Cell Rep. 2012;2(4):991-1001. Epub 20121011. doi: 10.1016/j.celrep.2012.09.011.
48. Öztürk-Çolak A, Marygold SJ, Antonazzo G, Attrill H, Goutte-Gattat D, Jenkins VK, et al. FlyBase: updates to the Drosophila genes and genomes database. Genetics. 2024;227(1). doi: 10.1093/genetics/iyad211.
49. Langmead B, Salzberg SL. Fast gapped-read alignment with Bowtie 2. Nat Methods. 2012;9(4):357-9. doi: 10.1038/nmeth.1923.
50. Danecek P, Bonfield JK, Liddle J, Marshall J, Ohan V, Pollard MO, et al. Twelve years of SAMtools and BCFtools. Gigascience. 2021;10(2). doi: 10.1093/gigascience/giab008.
51. Quinlan AR, Hall IM. BEDTools: a flexible suite of utilities for comparing genomic features. Bioinformatics. 2010;26(6):841-2. doi: 10.1093/bioinformatics/btq033.
52. Buenrostro JD, Giresi PG, Zaba LC, Chang HY, Greenleaf WJ. Transposition of native chromatin for fast and sensitive epigenomic profiling of open chromatin, DNA-binding proteins and nucleosome position. Nat Methods. 2013;10(12):1213-8. Epub 20131006. doi: 10.1038/nmeth.2688.

53. Zhang Y, Liu T, Meyer CA, Eeckhoute J, Johnson DS, Bernstein BE, et al. Model-based Analysis of ChIP-Seq (MACS). Genome Biology. 2008;9(9):R137. doi: 10.1186/gb-2008-9-9-r137.
54. Torres-Oliva M, Schneider J, Wiegleb G, Kaufholz F, Posnien N. Dynamic genome wide expression profiling of Drosophila head development reveals a novel role of Hunchback in retinal glia cell development and blood-brain barrier integrity. PLoS Genet. 2018;14(1):e1007180. Epub 20180123. doi: 10.1371/journal.pgen.1007180.
55. Bentsen M, Goymann P, Schultheis H, Klee K, Petrova A, Wiegandt R, et al. ATAC-seq footprinting unravels kinetics of transcription factor binding during zygotic genome activation. Nat Commun. 2020;11(1):4267. Epub 20200826. doi: 10.1038/s41467-020-18035-1.
56. Rauluseviciute I, Riudavets-Puig R, Blanc-Mathieu R, Castro-Mondragon JA, Ferenc K, Kumar V, et al. JASPAR 2024: 20th anniversary of the open-access database of transcription factor binding profiles. Nucleic Acids Res. 2024;52(D1):D174-D82. doi: 10.1093/nar/gkad1059.
57. Weirauch MT, Yang A, Albu M, Cote AG, Montenegro-Montero A, Drewe P, et al. Determination and inference of eukaryotic transcription factor sequence specificity. Cell. 2014;158(6):1431-43. doi: 10.1016/j.cell.2014.08.009.
58. Smith JM, Sondhi KC. The arrangement of bristles in Drosophila. J Embryol Exp Morphol. 1961;9:661-72.
59. Estella C, Mann RS. Logic of Wg and Dpp induction of distal and medial fates in the Drosophila leg. Development. 2008;135(4):627-36. Epub 20080109. doi: 10.1242/dev.014670.
60. Tavsanli BC, Ostrin EJ, Burgess HK, Middlebrooks BW, Pham TA, Mardon G. Structure-function analysis of the Drosophila retinal determination protein Dachshund. Dev Biol. 2004;272(1):231-47. doi: 10.1016/j.ydbio.2004.05.005.
61. Lin MC, Park J, Kirov N, Rushlow C. Threshold response of C15 to the Dpp gradient in Drosophila is established by the cumulative effect of Smad and Zen activators and negative cues. Development. 2006;133(24):4805-13. Epub 20061108. doi: 10.1242/dev.02689.
62. Del Signore SJ, Hayashi T, Hatini V. odd-skipped genes and lines organize the notum anterior-posterior axis using autonomous and non-autonomous mechanisms. Mech Dev. 2012;129(5-8):147-61. Epub 20120514. doi: 10.1016/j.mod.2012.05.001.
63. Hagen JFD, Mendes CC, Blogg A, Payne A, Tanaka KM, Gaspar P, et al. tartan underlies the evolution of Drosophila male genital morphology. Proc Natl Acad Sci U S A. 2019;116(38):19025-30. Epub 20190904. doi: 10.1073/pnas.1909829116.
64. Hagen JFD, Mendes CC, Booth SR, Figueras Jimenez J, Tanaka KM, Franke FA, et al. Unraveling the Genetic Basis for the Rapid Diversification of Male Genitalia between Drosophila Species. Mol Biol Evol. 2021;38(2):437-48. doi: 10.1093/molbev/msaa232.
65. Sakurai KT, Kojima T, Aigaki T, Hayashi S. Differential control of cell affinity required for progression and refinement of cell boundary during Drosophila leg segmentation. Dev Biol. 2007;309(1):126-36. Epub 20070710. doi: 10.1016/j.ydbio.2007.07.001.
66. Nagy O, Nuez I, Savisaar R, Peluffo AE, Yassin A, Lang M, et al. Correlated Evolution of Two Copulatory Organs via a Single cis-Regulatory Nucleotide Change. Curr Biol. 2018;28(21):3450-7 e13. Epub 20181018. doi: 10.1016/j.cub.2018.08.047.
67. Tanaka KM, Takahashi K, Rice G, Rebeiz M, Kamimura Y, Takahashi A. Trichomes on female reproductive tract: rapid diversification and underlying gene regulatory network in Drosophila suzukii and its related species. BMC Ecol Evol. 2022;22(1):93. Epub 20220728. doi: 10.1186/s12862-022-02046-1.
68. Yassin A, Orgogozo V. Coevolution between male and female genitalia in the Drosophila melanogaster species subgroup. PLoS One. 2013;8(2):e57158. Epub 20130225. doi: 10.1371/journal.pone.0057158.
69. Mattei AL, Riccio ML, Avila FW, Wolfner MF. Integrated 3D view of postmating responses by the Drosophila melanogaster female reproductive tract, obtained by micro-computed tomography scanning. Proc Natl Acad Sci U S A. 2015;112(27):8475-80. Epub 20150603. doi: 10.1073/pnas.1505797112.
70. Tanaka KM, Hopfen C, Herbert MR, Schlötterer C, Stern DL, Masly JP, et al. Genetic architecture and functional characterization of genes underlying the rapid diversification of male external genitalia between Drosophila simulans and Drosophila mauritiana. Genetics. 2015;200(1):357-69. Epub 20150316. doi: 10.1534/genetics.114.174045.
71. Chyb S, Gompel N. Atlas of Drosophila Morphology. San Diego: Academic Press; 2013.

72. Urum A, Rice G, Glassford W, Yanku Y, Shklyar B, Rebeiz M, Preger-Ben Noon E. A developmental atlas of male terminalia across twelve species of Drosophila. Front Cell Dev Biol. 2024;12:1349275. doi: 10.3389/fcell.2024.1349275.

Supplementary Figures

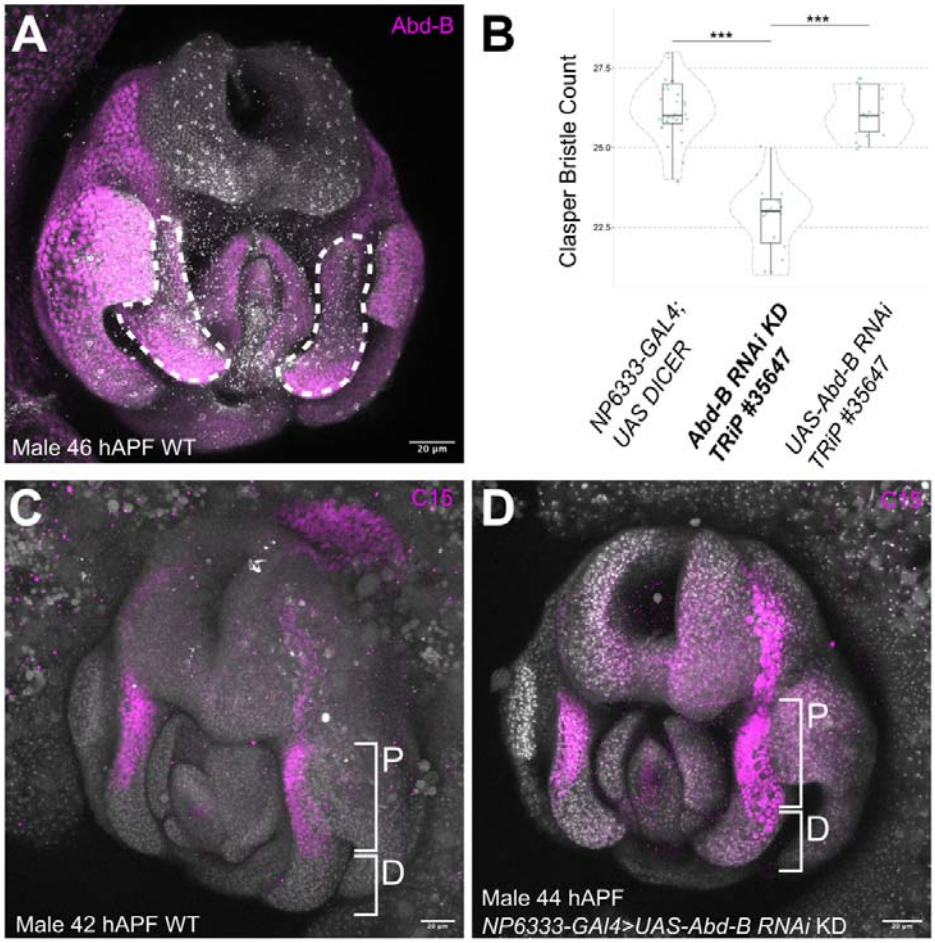

Supplementary Figure 1. Abd-B expression and regulation of *C15* in the developing male terminalia. (A) Abd-B is expressed throughout the entire male terminalia apart from the cerci. Dashed white lines mark the claspers. (B) RNAi knockdown of *Abd-B* significantly reduced clasper bristle count compared to parental controls. *** $p < 0.001$ ($n > 16$). (C) C15 expression pattern in late pupal male claspers. (D) RNAi knockdown of *Abd-B* slightly expanded C15 expression into the distal region of the clasper, as well as at the periphery of the cerci. P: Proximal, D: Distal clasper regions. All samples were DAPI stained, apart from (A), where anti-DCAD2 staining was used.

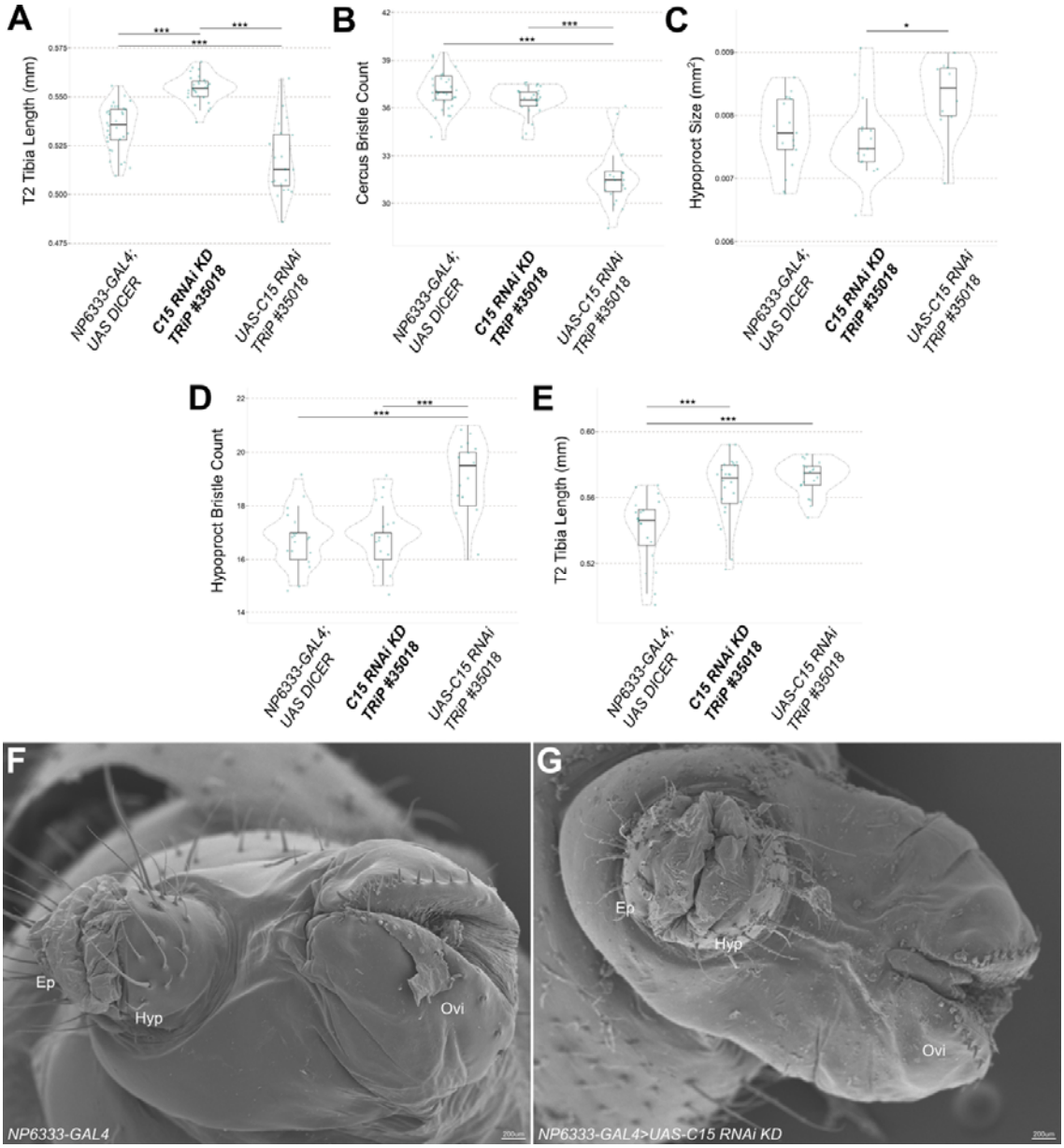

Supplementary Figure 2. *C15* RNAi knockdown in the developing male and female terminalia. (A) *C15* RNAi knockdown significantly increased male T2 tibia length. (B) *C15* RNAi knockdown did not affect male cercus bristle number. (C) In females, *C15* RNAi knockdown had no significant effect on the hypoproct size (C), hypoproct bristle count (D), or T2 tibia length (E). (F,F') SEM images of the adult female terminalia in *NP6333-GAL4* parental control (F) and *C15* RNAi knockdown (F'). Epi: Epiproct, Hyp: Hypoproct, Ovi: Ovipositor. *** $p < 0.001$, and * $p < 0.05$. $n > 9$, (Supplementary Tables 1 and 2).

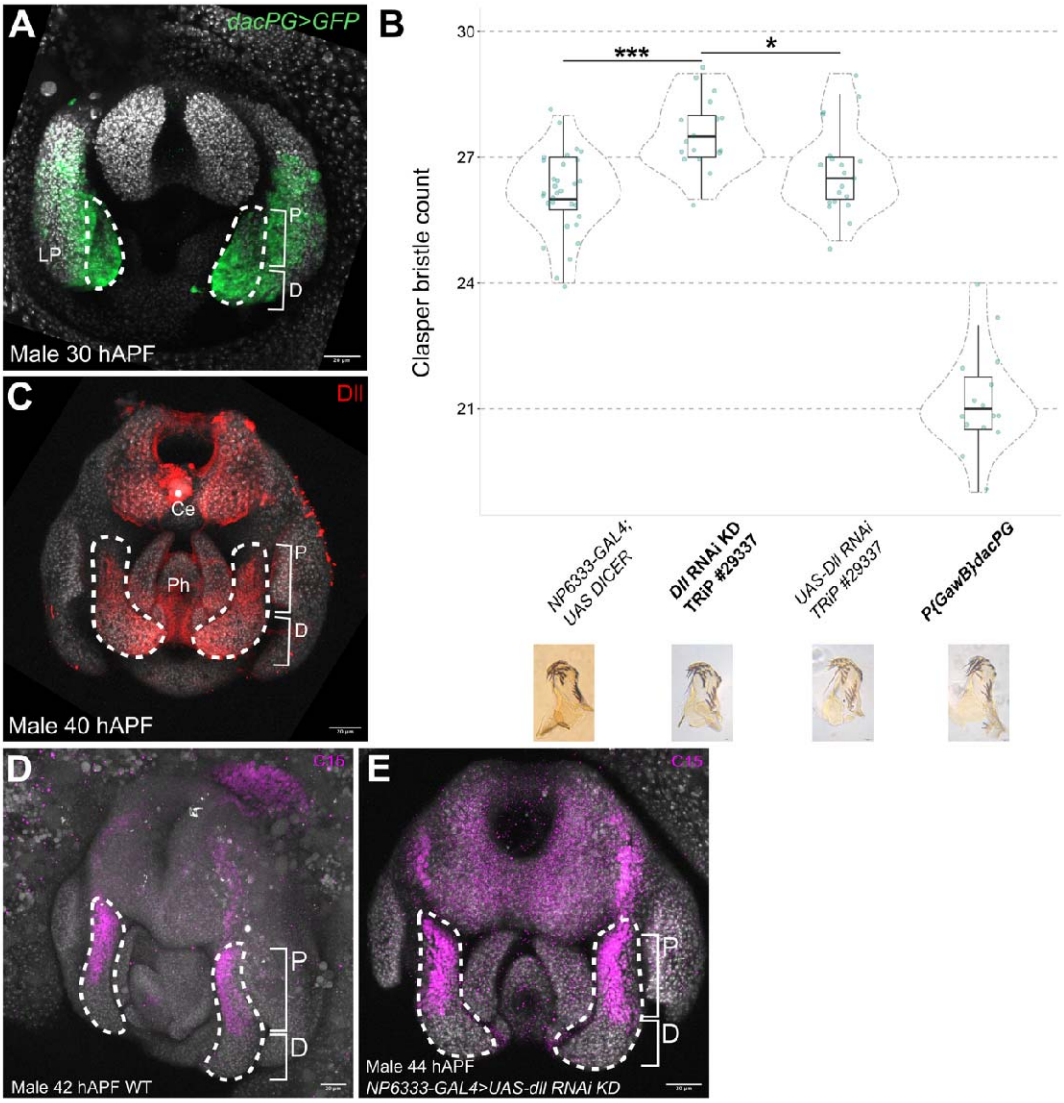

Supplementary Figure 3. Roles of Dac and Dll during male terminalia development.
(A) *dac* is expressed predominantly in the distal clasper regions and in the lateral plate (LP). (B) *Dll* and *dac* are both required for male clasper bristle development. The *P{GawB}dacPG* line could not be compared to other genotypes because one parental line was not available for analysis. *** $p < 0.001$, * $p < 0.05$ ($n > 16$ for all lines phenotyped) (Supplementary Table 1). (C) Dll is expressed throughout the claspers, and in part of the phallus, and cerci [31]. (D,E) *Dll* RNAi knockdown did not appear to alter C15 localization. P (proximal) and D (distal) clasper regions. LP: Lateral Plate, Ph: Phallus, Ce: Cercus.

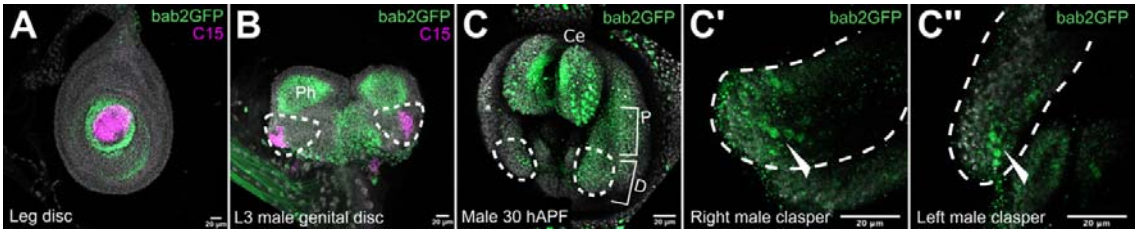

Supplementary Figure 4. *bab2* expression in developing male terminalia. (A) To verify if the GFP-tagged *bab2* transgenic line recapitulated endogenous *bab2* expression, the leg disc was double stained with anti-GFP and anti-C15. (B) In male genital discs, bab2-GFP localised to the phallus (Ph) and the repressed female primordium. No bab2-GFP expression was observed in the clasper primordia, as marked by C15. (C-C'') In male pupal terminalia, bab2-GFP was expressed throughout the cerci (Ce), as well as in the distal region of the clasper. All samples were stained with DAPI.

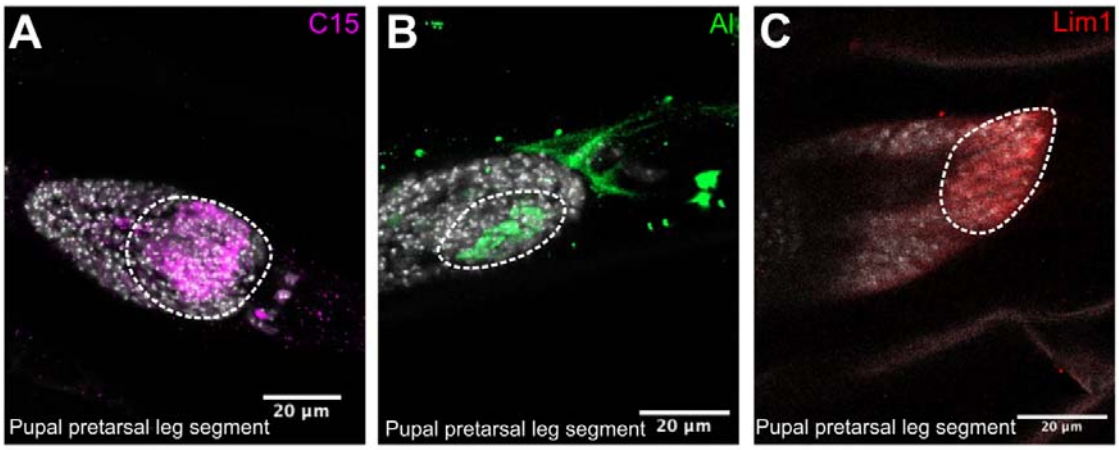

Supplementary Figure 5. Pupal pre-tarsal leg expression of C15, Al, and Lim1. (A) C15, (B) Al, and (C) Lim1 expression at the pretarsal segment of late pupae legs, where the claw protrudes from. White dashed ovals mark regions of expression. All samples were stained with DAPI.

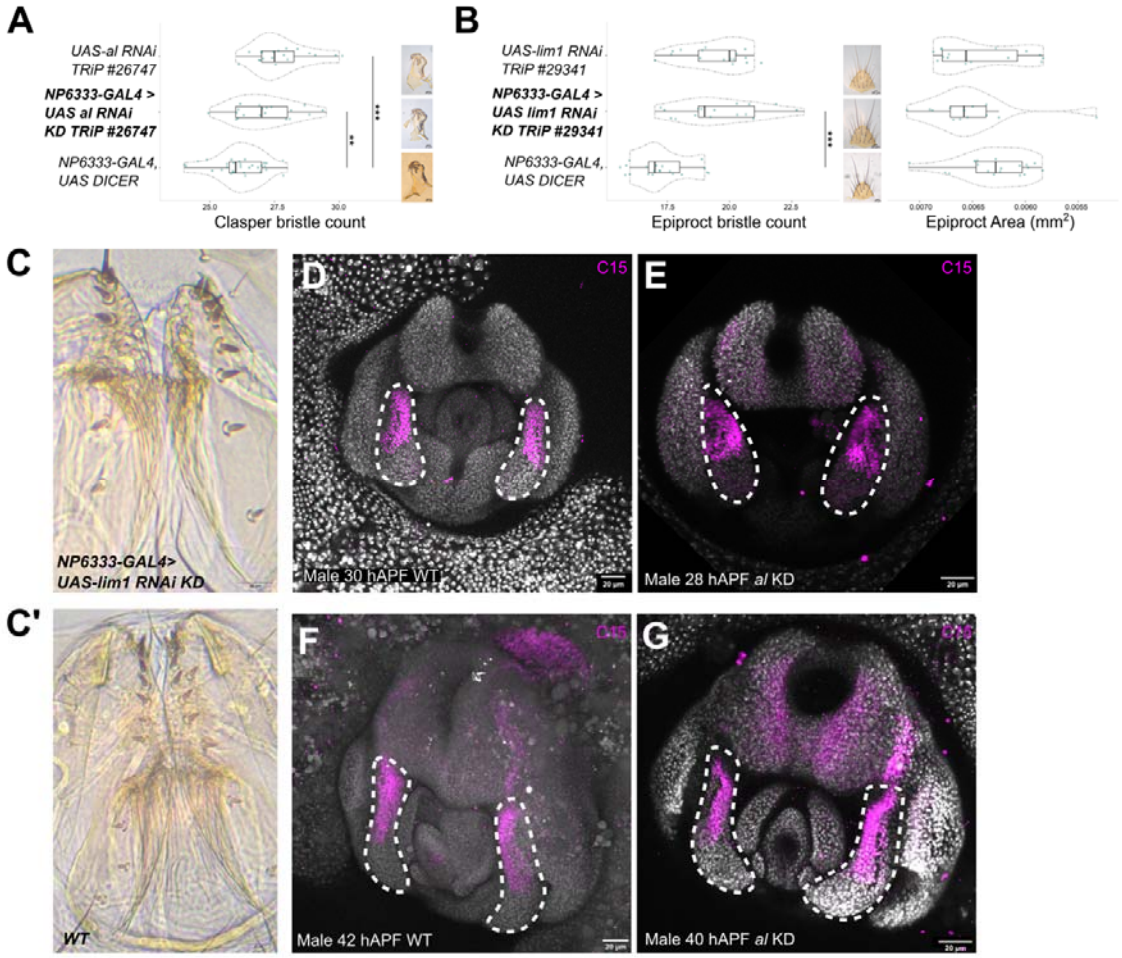

Supplementary Figure 6. Roles of Al and Lim1 during male and female terminalia development, respectively. (A) RNAi knockdown of *al* did not affect male clasper development. (B) RNAi knockdown of *Lim1* did not affect female epiproct development. (C) *Lim1* RNAi knockdown in the female ovipositor reduced the number of ovipositor teeth compared to wild-type female ovipositors (C'). (D) C15 is expressed in the proximal region of the developing male claspers. (E) RNAi knockdown of *al* did not affect C15 expression. (F) C15 expression is maintained at the proximal clasper region in late pupal development. (G) RNAi knockdown of *al* did not affect C15 expression. All samples were DAPI stained. *** $p < 0.001$, ** $p < 0.01$ (Supplementary Tables 1 and 2). $n > 14$ for all lines phenotyped.

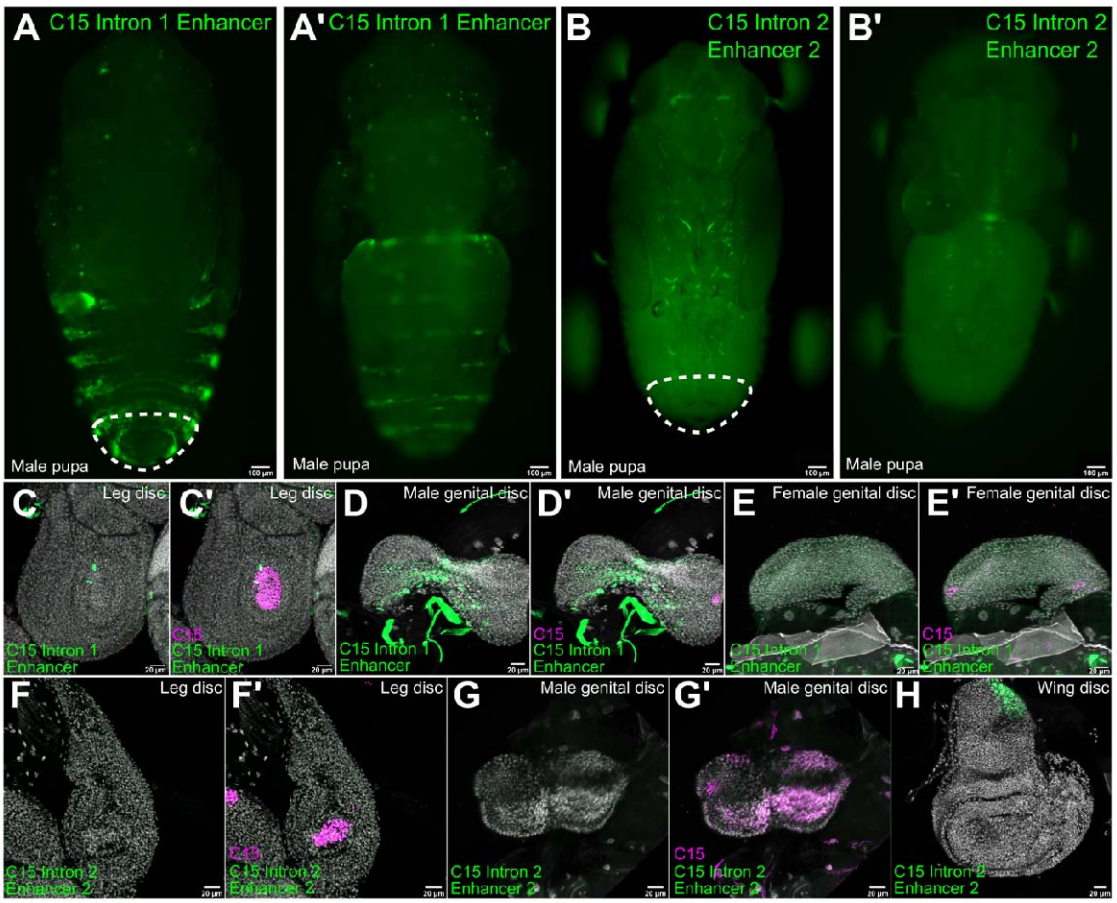

Supplementary Figure 7. *C15* intron 1 and intron 2 enhancer 2 activity during development. (A,A') Live imaging of *C15* intron1 enhancer when crossed to *UAS-GFP* in male pupae. *C15* intron 1 enhancer is active in a segmental pattern in the abdomen. It is also active in the tissue surrounding the male terminalia. (B,B') The *C15* intron 2 enhancer 2 is active in the antennae but no activity was observed in the male terminalia. (C,C') The *C15* intron 1 enhancer is active in a few cells of the central leg disc and partially overlaps with endogenous C15 expression. (D,D') This enhancer is also active in the repressed female primordium in the male genital disc but not in the female genital disc (E,E'). (F,F') The *C15* intron 2 enhancer 2 is not active in the leg disc, or the male genital disc (G,G'). (H) This enhancer is active in the notum of the wing disc where endogenous *C15* is expressed (See Figure 7). All samples were stained with DAPI.

Supplementary Tables

Supplementary Table 1. RNAi lines and male phenotypic results.

Supplementary Table 2. RNAi lines and female phenotypic results.

Supplementary Table 3. Antibodies used in this study.

Supplementary Table 4. Transcription factor binding sites predicted by CIS-BP.

Supplementary Table 5. Transcription factor binding sites predicted by JASPAR.